Kinetics of Emulsion Copolymerization with Acrylic Acids

GLENN L. SHOAF and GARY W. POEHLEIN*

School of Chemical Engineering, Georgia Institute of Technology, Atlanta, Georgia 30332-0100

SYNOPSIS

A kinetic model is presented that describes the reaction behavior of emulsion copolymerization systems where significant polymerization occurs in both the particle and aqueous phases. Equations for predicting aqueous-phase free-radical concentrations and aqueous-phase and particle-phase reaction rates are developed. A method for estimating the radical entry rate coefficient is also presented. The model is applied to two seeded carboxylated emulsion copolymerization systems, acrylic acid–styrene and methacrylic acid–styrene. Both experimental and predicted results reveal that the reaction behavior is greatly affected by the type of acid monomer, partition of monomer between the various phases, and locus of polymerization. The mechanism for the acrylic acid–styrene system is more complicated than that for the methacrylic acid–styrene system. Evidence suggests that the primary reaction locus in the acrylic acid–styrene system shifts from the particles to the aqueous phase after the hydrophobic monomer, styrene, has been consumed.

INTRODUCTION

Conventional emulsion polymer systems employ monomers that are relatively water insoluble such as styrene. The primary reaction locus is inside the polymer particles and aqueous-phase polymerization is usually negligible. Many industrial reaction systems, however, employ one or more monomers that have significant water solubility. The concentration and reaction of these monomers in the aqueous phase may be significant, and conventional emulsion polymerization kinetics do not apply to these systems.

Carboxylated copolymer latexes comprise an increasingly important class of industrial emulsion polymer systems involving water-soluble monomers. They are used widely for the production of paper coatings, textile coatings, and adhesives. Carboxylic acid monomers are often completely soluble in water. However, they will still distribute to varying extents into the organic phase depending on their relative hydrophobicity. Significant amounts of polymerization can occur in both the particle and aqueous phases.

* To whom correspondence should be addressed.

Journal of Applied Polymer Science, Vol. 42, 1213–1237 (1991)
 CCC 0021-8995/91/051213-25$04.00

Copolymerization Studies of Hydrophobic Monomers (i.e., Styrene) with Carboxylic Acid Monomers

Potentiometric and conductometric titration studies of copolymer latex systems containing acid monomers copolymerized with a more hydrophobic monomer such as styrene have been performed by a variety of workers including Fordyce and Ham,[1] Muroi,[2] Ceska,[3,4] Sakota and Okaya,[5] Vijayendran,[6] Egusa and Makuuchi,[7] and Gasper and Tan.[8] Most of these studies were aimed at determining the distribution of the acid groups between the aqueous phase, particle surface, and particle interior and the effects of these distributions on the rate of polymerization, particle stability, and particle generation.

The most frequently studied acid monomers copolymerized with styrene (or other hydrophobic monomers) are itaconic acid (IA), acrylic acid (AA), and methacrylic acid (MAA), listed in order of increasing hydrophobic nature. The amount of acid found buried inside the particle core increases with hydrophobicity of the monomer. Hydrophobic monomers diffuse into the particle, polymerize, and become a part of the particle core more easily than hydrophilic monomers. Hydrophilic acid monomers such as IA must be carried to the particle surface by oligomeric radicals that have polymerized in the

aqueous phase.[3] Very little IA monomer normally becomes incorporated within the particle core. The concentration of IA in the free aqueous phase is, therefore, greater than MAA when equal amounts are charged. The incorporation of AA into the particle core is intermediate between IA and MAA.[2,6-9]

Ceska copolymerized IA, AA, and MAA with styrene in separate reactions. Copolymerization rates were found to increase with the presence of carboxylic monomers in the order IA < AA < MAA.[2,3] The rate increased as the hydrophobicity of the monomer increased. The increase in overall reaction rate with hydrophobicity of the acid monomer may be related to two factors. First, the more hydrophobic acid monomers may become incorporated earlier in the reaction and thus stabilize a greater number of particles. Second, the more hydrophobic acid monomer partitions to a greater extent into the particles where the reaction rate is fastest.

Seeded reactions were utilized in this study in order to study the kinetics of carboxylated styrene emulsion systems without the complicated particle nucleation phenomena. A constant particle number was maintained by using a large concentration of seed particles to capture oligomers before significant secondary nucleation could occur. Small amounts of surfactant were used to stabilize existing particles while minimizing the chances for further particle nucleation. Examination of reaction samples with a transmission electron microscope revealed no signs of secondary nucleation under the conditions used in this study.

THEORY

Emulsion Copolymerization Kinetics

The basic initiation and propagation reactions for copolymerization of two monomers, M_A and M_B, are shown below.

Initiator decomposition

$$I \xrightarrow{k_d} 2R^*$$

Monomer initiation

$$R^* + M_{A_1} \xrightarrow{k_{iA}} M^*_{A_1}$$

$$R^* + M_{B_1} \xrightarrow{k_{iB}} M^*_{B_1}$$

$$R^* + \text{impurities} \rightarrow \text{inactive product}$$

Propagation

$$M^*_{A_j} + M_{A_1} \xrightarrow{k_{pAA}} M^*_{A_{j+1}}$$

$$M^*_{A_j} + M_{B_1} \xrightarrow{k_{pAB}} M^*_{B_{j+1}}$$

$$M^*_{B_j} + M_{A_1} \xrightarrow{k_{pBA}} M^*_{A_{j+1}}$$

$$M^*_{B_j} + M_{B_1} \xrightarrow{k_{pBB}} M^*_{B_{j+1}}$$

Monomer chain transfer

$$M^*_{A_k} + M_{A_1} \xrightarrow{k_{trAA}} M_{A_k} + M^*_{A_1}$$

$$M^*_{A_k} + M_{B_1} \xrightarrow{k_{trAB}} M_{A_k} + M^*_{B_1}$$

$$M^*_{B_k} + M_{A_1} \xrightarrow{k_{trBA}} M_{B_k} + M^*_{A_1}$$

$$M^*_{B_k} + M_{B_1} \xrightarrow{k_{trBB}} M_{B_k} + M^*_{B_1}$$

Termination

$$M^*_{A_j} + M^*_{A_k} \xrightarrow{k_{tAA}} \text{dead polymer}$$

$$M^*_{A_j} + M^*_{B_k} \xrightarrow{k_{tAB}} \text{dead polymer}$$

$$M^*_{B_j} + M^*_{B_k} \xrightarrow{k_{tBB}} \text{dead polymer}$$

j refers to the number of monomer units of either type A or B in the oligomeric chain, whereas the A or B refers only to the type of monomer unit at the end of the chain.

It is unlikely that initiator radicals will be found inside the particles since they are most likely to react before entering a polymer particle. The chain transfer reactions are most important in the particle phase since the formation of single monomer radicals may lead to the exit or "desorption" of radicals from the particles. The rate of entry and exit of free radicals significantly affects the concentration of radicals in the particles and in the aqueous phase and thus the rates of reaction in each phase.

Nomura et al.[10] developed rate equations for emulsion copolymerization inside the polymer particles. Eqs. (1), (2), and (3) give the reaction rates for monomer A, monomer B, and total monomer, respectively.

$$R_{pA} = -dM_A/dt = k_{pAA}[M_A]_p N_{A^*} + k_{pBA}[M_A]_p N_{B^*} \quad (1)$$

$$R_{pB} = -dM_B/dt = k_{pBB}[M_B]_p N_{B^*} + k_{pAB}[M_B]_p N_{A^*} \quad (2)$$

$$R_{ptot} = R_{pA} + R_{pB} \quad (3)$$

where N_{A^*} and N_{B^*} are the number of particles per volume of water containing A and B radicals, respectively. Note that eqs. (1) and (2) do not include polymerization in the aqueous phase.

Nomura et al.[10] used eq. (4) to express the composition of copolymer formed in the particles.

$$\frac{dM_A}{dM_B} = \frac{[M_A]_p(r_A[M_A]_p + [M_B]_p)}{[M_B]_p(r_B[M_B]_p + [M_A]_p)} \quad (4)$$

They also assumed that the change in concentration of A^* and B^* radicals with time is slow when compared to the time scale of the complete reaction. Hence,

$$k_{pBA}[M_A]N_{B^*} = k_{pAB}[M_B]N_{A^*} \quad (5)$$

They then defined an average number of respective radicals per particle.

$$\bar{n}_A = N_{A^*}/N_T, \quad \bar{n}_B = N_{B^*}/N_T, \quad \bar{n}_I = N_{I^*}/N_T$$

and

$$\bar{n}_t = (N_{A^*} + N_{B^*} + N_{I^*})/N_T$$

where N_{I^*} is the number of particles containing an initiator radical.

The number of initiator radicals is relatively small, and when water-soluble initiators are used, these radicals are not likely to enter the hydrophobic polymer particles so that

$$\bar{n}_t = \bar{n}_A + \bar{n}_B + \bar{n}_I \cong \bar{n}_A + \bar{n}_B \quad (6)$$

$\bar{n}$ may be calculated using a procedure developed by Ugelstad and Hansen[11] that involves the method of continuous fractions.

After various algebraic manipulations, copolymerization rates can be written.

$$R_{pA} = \frac{[1/(1+A)](k_{pAA}[M_A]_p + k_{pAB}[M_B]_p)\bar{n}_t N_p}{N_A} \quad (7)$$

$$R_{pB} = \frac{[A/(1+A)](k_{pBA}[M_A]_p + k_{pBB}[M_B]_p)\bar{n}_t N_p}{N_A} \quad (8)$$

where

$$A = \frac{\bar{n}_B}{\bar{n}_A} = \frac{k_{pAA}}{k_{pBB}}\frac{r_B}{r_A}\frac{[M_B]_p}{[M_A]_p} \quad (9)$$

Aqueous-Phase Free-Radical Concentration in Emulsion Copolymerization Systems

Emulsion copolymerization, which includes at least one monomer with a high degree of water solubility, probably involves a significant amount of reaction in the aqueous phase. A kinetic model of emulsion copolymerization for these types of systems requires that the concentration of free radicals in the aqueous phase be known. A useful expression for obtaining the aqueous-phase free-radical concentration developed in collaboration with Mead[12] can be derived by the following method.

Reactions affecting all aqueous-phase radical species are listed in Table I. Corresponding rate expressions are also shown. An expression for the rate of change of initiator free-radical species can be written as follows:

$$\frac{d[I^*]}{dt} = \text{rate of formation by decomposition of } I_2$$
$$- \text{rate of monomer initiation}$$
$$- \text{rate of termination with other } I^* \text{ radicals}$$
$$- \text{rate of termination with oligomer radicals}$$
$$- \text{rate of capture by particles}$$
$$+ \text{rate of desorption from particles}$$
$$- \text{rate of capture by monomer droplets}$$
$$- \text{rate of capture by micelles}$$

Due to the high concentration of monomer relative to the concentration of initiator radicals, it is unlikely that termination between two initiator radicals will occur. The initiator free radical is very reactive and has a short lifetime. Therefore, the third and last four terms of the previous expression may be neglected. The resulting expression is given by

Table I Reactions Affecting Aqueous-Phase-Radical Species

1.	• decomposition	$I_2 \xrightarrow{k_D} 2I^*$	$R_d = 2fk_d[I_2]$
2a.	• monomer initiation	$I^* + A_w \xrightarrow{k_{IA}} R_{1A^\bullet}$	$R_{IA} = k_{IA}[A]_w[I^*]$
2b.		$I^* + B_w \xrightarrow{k_{IB}} R_{1B^\bullet}$	$R_{IB} = k_{IB}[B]_w[I^*]$
3.	• deactivation	$I^* +$ impurities $\rightarrow$ dead prod	$R_{deac} = 2(1-f)k_d[I_2]$
4a.	• termination	$I^* + I^* \xrightarrow{k_{twII}} I_2$	$R_{twII} = 2k_{twII}[I^*]^2$
4b.		$I^* + R^*_{jA} \xrightarrow{k_{twIA}} I - R^*_{jA}$	$R_{term} = 2k_{twIA}[R^*_{jA}][I^*]$
4c.		$I^* + R^*_{jB} \xrightarrow{k_{twIB}} I - R^*_{jB}$	$R_{term} = 2k_{twIB}[R^*_{jB}][I^*]$
5a.	• propagation	$R^*_{jA} + A_w \xrightarrow{k_{pAA}} R^*_{j+1A}$	$R_{pAA} = k_{pAA}[R^*_{jA}][A]_w$
5b.		$R^*_{jA} + B_w \xrightarrow{k_{pAB}} R^*_{j+1B}$	$R_{pAB} = k_{pAA}[R^*_{jA}][B]_w$
5c.		$R^*_{jB} + A_w \xrightarrow{k_{pBA}} R^*_{j+1A}$	$R_{pBA} = k_{pBA}[R^*_{jB}][A]_w$
5d.		$R^*_{jB} + B_w \xrightarrow{k_{pBB}} R^*_{j+1B}$	$R_{pBB} = k_{pBB}[R^*_{jB}][B]_w$
6a.	• capture of init.	$I^* + P \xrightarrow{k_{cI}} P^*_I$	$R_{cI} = k_{cI}N_p[I^*]$
6b.	and oligomer radi-	$R^*_{jA} + P \xrightarrow{k_{cjA}} P^*_A$	$R_{cA} = k_{cjA}N_p[R^*_{jA}]$
6c.	cals by particles	$R^*_{jB} + P \xrightarrow{k_{cjB}} P^*_B$	$R_{cB} = k_{cjB}N_p[R^*_{jB}]$
7a.	• desorption of	$P^*_I \xrightarrow{k_{desI}} I^* + P$	$R_{desI} = k_{desI}(N_p\bar{n}/N_A)$
7b.	radicals from	$P^*_A \xrightarrow{k_{desA}} R^*_{jA} + P$	$R_{desA} = k_{desA}(N_p\bar{n}/N_A)$
7c.	particles	$P^*_B \xrightarrow{k_{desB}} R^*_{jB} + P$	$R_{desB} = k_{desB}(N_p\bar{n}/N_A)$
8a.	• termination of	$R^*_{iA} + R^*_{jA} \xrightarrow{k_{twAA}} O_{i+j}$	$R_{term} = 2k_{twAA}[R^*]^2$
8b.	oligomer radicals	$R^*_{iA} + R^*_{jB} \xrightarrow{k_{twAB}} O_{i+j}$	$R_{term} = 2k_{twAB}[R^*_{iA}][R^*_B]$
8c.		$R^*_{iB} + R^*_{jB} \xrightarrow{k_{twBB}} O_{i+j}$	$R_{term} = 2\bar{k}_{twBB}[R^*_B]^2$
9a.	• capture of	$I^* + D \xrightarrow{k_{cDI}} P^*_{DI}$	$R_{cDI} = k_{cDI}N_D[I^*]$
9b.	radicals by	$R^*_{jA} + D \xrightarrow{k_{cDA}} P^*_{DA}$	$R_{cDA} = k_{cDA}N_D[R^*_{jA}]$
9c.	droplets	$R^*_{jB} + D \xrightarrow{k_{cDB}} P^*_{DB}$	$R_{cDB} = k_{cDB}N_D[R^*_{jB}]$
10a.	• capture of	$I^* + M_c \xrightarrow{k_{McI}} P^*_{MI}$	$R_{MCI} = k_{MCI}N_{MC}[I^*]$
10b.	radicals by	$R^*_{jA} + M_c \xrightarrow{k_{McA}} P^*_{MA}$	$R_{MCA} = k_{MCA}N_{MC}[R^*_{jA}]$
10c.	micelles	$R^*_{jB} + M_c \xrightarrow{k_{McB}} P^*_{MB}$	$R_{MCB} = k_{MCB}N_{MC}[R^*_{jB}]$

$$\frac{d[I^*]}{dt} = 2fk_d[I_2] - 2k_{IA}[A]_w[I^*] + 2k_{IB}[B]_w[I^*] - 2k_{twI}[R^*_{tot}][I^*] \quad (10)$$

A balance on the monomer radicals ($j = 1$) is given below.

$$\frac{d[R^*_1]}{dt} = \text{rate of initiation of monomer molecules}$$

$-$ rate of formation of $j = 2$ mers

$-$ rate of termination with initiator radicals

$-$ rate of termination with oligomer radicals

$-$ rate of capture by particles

$-$ rate of capture by drops, micelles

$+$ rate of desorption from particles

Capture by monomer droplets is usually negligible, and if the surfactant level is kept below its critical micelle concentration, micelles will not be present in the system. Applying the assumption that the identity of a radical A^* or B^* is independent of chain length gives

$$R^*_{1A} = \frac{R^*_1}{1 + A_w} \quad (11)$$

$$R^*_{1B} = \frac{A_w R^*_1}{1 + A_w} \quad (12)$$

A_w is a term introduced by Nomura that assumes that the probability of a radical ending with an A^* or B^* unit is independent of chain length, and that the rate of change in the proportion of the radicals is small over the course of the reaction period. A_w is defined by

$$A_w = \frac{[R^*_{jB}]}{[R^*_{jA}]} = \frac{k_{pAA}}{k_{pBB}} \frac{r_B}{r_A} \frac{[B]_w}{[A]_w} \tag{13}$$

The rate expression for the monomer radicals can then be written by

$$\frac{d[R^*_1]}{dt} = (k_{IA}[A]_w + k_{IB}[B]_w)[I^*] - \frac{R_{1^*}}{1 + A_w}[(k_{pAA} + A_w k_{pBA})[A]_w + (k_{pAB} + A_w k_{pBB})[B]_w] - 2\bar{k}_{twI}[R_{1^*}][I^*] - 2\bar{k}_{tw}[R_{1^*}][R^*_{\text{tot}}] - \bar{k}_{c1}[R_{1^*}]N_p + \bar{k}_{\text{des}}(N_p\bar{n}/N_a) \tag{14}$$

where the average constants and overall radical concentration are given by the following expressions:

$$\bar{k}_{twI} = \frac{[R^*_{jA}]k_{twIA} + [R^*_{jB}]k_{twIB}}{[R^*_{jA}] + [R^*_{jB}]} \tag{15}$$

$$\bar{k}_{tw} = \frac{1}{(1 + A_w)^2}(k_{twAA} + A_w k_{twAB} + A_w^2 k_{twBB}) \tag{16}$$

$$\bar{k}_{c1} = \frac{k_{c1A}[R^*_{1A}] + k_{c1B}[R^*_{1B}]}{[R^*_{1A}] + R^*_{1B}]} \tag{17}$$

Next, a balance is written on the j-mer radicals with $j > 1$.

$$\frac{d[R_{j^*}]}{dt} = \text{rate of formation of } j\text{-mer} - \text{rate of formation of } j+1 \text{ mer} - \text{rate of termination with initiator radicals} - \text{rate of termination with oligomer radicals} - \text{rate of capture by particles} - \text{rate of capture by drops, micelles} + \text{rate of desorption from particles}$$

Again, capture by droplets and micelles is neglected relative to capture by seed particles. Desorption from latex particles is also unlikely if j is much larger than 1. The resulting rate expression is given by eq. (18). [Note that eq. (15) has been extended to include radicals of length j.]

$$\frac{d[R^*_j]}{dt} = \frac{[R^*_j]}{1 + A_w}[(k_{pAA} + A_w k_{pBA})[A]_w + (k_{pAB} + A_w k_{pBB})[B]_w] - \frac{[R^*_{j+1}]}{1 + A_w}[(k_{pAA} + A_w k_{pBA})[A]_w + (k_{pAB} + A_w k_{pBB})[B]_w] - 2\bar{k}_{twI}[R^*_j][I^*] - 2\bar{k}_{tw}[R^*_j][R^*_{\text{tot}}] - \bar{k}_{cj}[R^*_{j^*}]N_p \tag{18}$$

where

$$\bar{k}_{cj} = \frac{[R^*_{jA}]k_{cjA} + [R^*_{jB}]k_{cjB}}{[R^*_{jA}] + [R^*_{jB}]} \tag{19}$$

$$[R^*_j] = [R^*_{jA}] + [R^*_{jB}] \tag{20}$$

The oligomers grow to a critical length beyond which capture by particles is assumed to occur. This critical length is denoted by j_{cr}. Therefore, the system of equations developed consists of j_{cr} equations. The steady-state assumption must be applied in order to solve the j_{cr} system of equations. The derivatives are all set to zero and the j_{cr} equations are summed yielding

$$2fk_d[I_2] - 2\bar{k}_{twI}[R^*_{\text{tot}}][I^*] - 2\bar{k}_{tw}\sum_{j=1}^{j_{\text{cr}}-1}[R^*_j][R^*_{\text{tot}}] - N_p\sum_{j=1}^{j_{\text{cr}}-1}\bar{k}_{cj}[R^*_j] + \bar{k}_{\text{des}}\left(\frac{N_p\bar{n}}{N_A}\right) - \frac{[R^*_{j\text{cr}-1}]}{1 + A_w}[(k_{pAA} + A_w k_{pBA})[A]_w + (k_{pAB} + A_w k_{pBB})[B]_w] = 0 \tag{21}$$

One may then define $\bar{k}_c$, an average radical capture constant, as was done by Ugelstad and Hansen.[11]

$$\bar{k}_c = \sum_{j=1}^{j_{\text{cr}}-1}\frac{k_{cj}[R^*_j]}{[R^*_{\text{tot}}]} \tag{22}$$

and rewrite the expression for the average termination constant,

$$2\bar{k}_{tw}\sum_{j=1}^{j_{\text{cr}}-1}[R^*_j][R^*_{\text{tot}}] = 2\bar{k}_{tw}[R^*_{\text{tot}}]^2 \tag{23}$$

A more simplified equation then follows:

$$2fk_d[I_2] - 2\bar{k}_{twI}[R^*_{tot}][I^*] - 2\bar{k}_{tw}[R^*_{tot}]^2 - \bar{k}_c N_p[R^*_{tot}] + \bar{k}_{des}\left(\frac{N_p\bar{n}}{N_a}\right) - \frac{[R^*_{jcr-1}]}{1+A_w}[(k_{pAA} + A_w k_{pBA})[A]_w + (k_{pAB} + A_w k_{pBB})[B]_w] = 0 \quad (24)$$

This equation is of the same form as that derived by Ugelstad and Hansen[11] for homopolymerization. Two additional assumptions can be made to simplify this expression.

1. If seed is present, flocculation of oligomers onto seed particles should be great enough that few oligomer species can reach the critical chain length needed for homogeneous nucleation of particles. Therefore, $[R^*_{jcr-1}]$ should be very small (especially compared to $[R^*_{tot}]$), and the last term can be neglected.
2. If the initiator is very reactive (i.e., potassium persulfate), and if the concentration of monomer(s) in the aqueous phase is significant (i.e., significantly water-soluble monomers such as carboxylic acids), $[I^*]$ should be small, and the second term can also be neglected.

These simplifications lead to

$$2fk_d[I_2] - 2\bar{k}_{tw}[R^*_{tot}]^2 - \bar{k}_c N_p[R^*_{tot}] + \bar{k}_{des}(N_p\bar{n}/N_A) = 0 \quad (25)$$

Application of the quadratic formula leads to a direct solution for $[R^*_{tot}]$.

$$[R^*_{tot}] = \frac{\sqrt{(\bar{k}_c N_p)^2 + 8\bar{k}_{tw}(\bar{k}_{des}N_p\bar{n}/N_a + 2fk_d[I_2])} - \bar{k}_c N_p}{4\bar{k}_{tw}} \quad (26)$$

Expression for Diffusion-Controlled Aqueous-Phase Copolymerization

The rationale used in the previous derivation of $[R^*_{tot}]$ can be used in deriving an expression for diffusion-controlled aqueous-phase copolymerization in an emulsion system. The rate expression is given by

$$R_{paq} = -\frac{(d[A]_{aq} + d[B]_{aq})}{dt} = k_{pAA}[A^*]_{aq}[A]_{aq} + k_{pAB}[A^*]_{aq}[B]_{aq} + k_{pBA}[B^*]_{aq}[A]_{aq} + k_{pBB}[B^*]_{aq}[B]_{aq} \quad (27)$$

A steady-state concentration is assumed for each type of radical.

$$k_{pBA}[B^*]_{aq}[A]_{aq} = k_{pAB}[A^*]_{aq}[B]_{aq} \quad (28)$$

Steady state is also assumed for the total concentration of radicals, which normally leads to an expression of the form

$$R_{initiation} = R_{termination} \quad (29)$$

However, as shown in the previous discussion involving an emulsion system, radical capture by latex particles and radical desorption from latex particles are important. Therefore, eq. (29) must be modified to

$$R_{initiation} = R_{termination} + R_{capture} - R_{desorption} \quad (30)$$

which leads to

$$R_i = 2\bar{k}_{tw}([A^*]_{aq} + [B^*]_{aq})^2 + \bar{k}_c([A^*]_{aq} + [B^*]_{aq})N_p - \bar{k}_{des}(N_p\bar{n}/N_A) \quad (31)$$

Rearranging and solving for the free radical concentration gives

$$[A^*]_{aq} + [B^*]_{aq} = [R^*_{tot}]_{aq} = \frac{\sqrt{(\bar{k}_c N_p)^2 + 8\bar{k}_{tw}(R_i + \bar{k}_{des}(N_p\bar{n}/N_A))} - \bar{k}_c N_p}{4\bar{k}_{tw}} \quad (32)$$

Solving for $[B^*]_{aq}$ from eq. (28) yields

$$[B^*]_{aq} = \frac{k_{pAB}[A^*]_{aq}[B]_{aq}}{k_{pBA}[A]_{aq}} \quad (33)$$

and substituting this result into eq. (32) and rearranging gives an expression for $[A^*]_{aq}$:

$$[A^*]_{aq} = \frac{\sqrt{(\bar{k}_c N_p)^2 + 8\bar{k}_{tw}(R_i + \bar{k}_{des}N_p\bar{n}/N_A)} - \bar{k}_c N_p}{4\bar{k}_{tw}(1 + k_{pAB}[B]_{aq}/k_{pBA}[A]_{aq})} \quad (34)$$

Let $r_A = k_{pAA}/k_{pAB}$ and $r_B = k_{pBB}/k_{pBA}$. Then substituting eqs. (33) and (34) into eq. (27) and rearranging leads to an expression for the rate of reaction in the aqueous phase.

$$R_{paq} = \frac{\sqrt{(\bar{k}_c N_p)^2 + 8\bar{k}_{tw}(R_i + \bar{k}_{des} N_p \bar{n}/N_A)} - \bar{k}_c N_p)}{4\bar{k}_{tw}(r_a[A]_{aq}/k_{pAA} + r_B[B]_{aq}/k_{pBB})} \times (r_A[A]_{aq}^2 + 2[A]_{aq}[B]_{aq} + r_B[B]_{aq}^2) \quad (35)$$

Separate expressions for each monomer can be derived for the aqueous-phase copolymerization rate. These expressions are more useful than eq. (35) for calculating the aqueous-phase copolymer composition. The derivation begins with eq. (27). Again, the steady-state assumption for the total concentration of free radicals and the assumption that the identity of an A^* or B^* radical is independent of chain length leads to

$$k_{pBA}[B^*]_{aq}[A]_{aq} = k_{pAB}[A^*]_{aq}[B]_{aq} \quad (36)$$

By definition,

$$A = \frac{[B^*]_{aq}}{[A^*]_{aq}} = \frac{k_{pAB}}{k_{pBA}} \frac{[B]_{aq}}{[A]_{aq}} \quad (37)$$

The total aqueous-phase concentration is equivalent to the sum of each type of free-radical species.

$$[R_{tot}]_{aq} = [A^*]_{aq} + [B^*]_{aq} \quad (38)$$

Algebraic manipulation of eqs. (37) and (38) lead to expressions for $[A^*]_{aq}$ and $[B^*]_{aq}$.

$$[A^*]_{aq} = \frac{1}{1+A}[R^*_{tot}]_{aq} \quad (39)$$

$$[B^*]_{aq} = \frac{A}{1+A}[R^*_{tot}]_{aq} \quad (40)$$

Breaking eq. (27) into two parts leads to

$$R_{p_{Aaq}} = k_{pAA}[A^*]_{aq}[A]_{aq} + k_{pBA}[B^*]_{aq}[A]_{aq} \quad (41)$$

$$R_{p_{Baq}} = k_{pAB}[A^*]_{aq}[B]_{aq} + k_{pBB}[B^*]_{aq}[B]_{aq} \quad (42)$$

Finally, substitution of eqs. (39) and (40) into eqs. (41) and (42) and rearrangement yield reaction rate expressions for the aqueous phase in terms of measurable parameters where $[R^*_{tot}]_{aq}$ is given by eq. (26).

$$R_{p_{Aaq}} = \frac{k_{pAA} + Ak_{pBA}}{1+A}[R^*_{tot}]_{aq}[A]_{aq} \quad (43)$$

$$R_{p_{Baq}} = \frac{k_{pAB} + Ak_{pBB}}{1+A}[R^*_{tot}]_{aq}[B]_{aq} \quad (44)$$

The overall emulsion copolymerization model then takes the form

$$R_{ptot} = R_{pAp} + R_{pBp} + R_{p_{Aaq}} + R_{p_{Baq}} \quad (45)$$

where the equations for rate of reaction in the particles are given by eqs. (7) and (8).

Transport of Radicals Out of Particles

Transport of free radicals from polymer particles, commonly referred to as radical desorption, is an important phenomenon in emulsion polymerization. The rate of transport of free radicals from particles greatly affects the free-radical concentration in both the particle and aqueous phases and thus affects the rate of reaction in each phase. The transport of free radicals to and from the particles was accounted for by Smith and Ewart[13] in their original recursion equation reproduced here.

$$N_n[\rho_a/N + nk_{des} + n(n-1)k_t/V_p] = N_{n-1}(\rho_a/N) + (n+1)k_{des}N_{n+1} + (n+2)(n+1)(k_t/V_p)N_{n+2} \quad (46)$$

where $N = \sum_{n=0}^{\infty} N_n$, and N_n is the number of polymer particles per unit volume of aqueous phase that contains n free radicals, ρ_a is the overall rate of radical absorption by the particles, V_p is the particle volume, k_{des} is a rate coefficient for radical desorption from the particles, and k_t is the radical termination constant in the particles.

Expressions for predicting the radical desorption coefficient, k_{des}, for homopolymerization systems have been developed by Ugelstad and co-workers,[11,14,15] and Nomura and co-workers.[16–18] Nomura et al.[10] then developed expressions for predicting an average radical desorption coefficient, $\bar{k}_{des}$, for an emulsion copolymerization system. Nomura developed eq. (47) to predict the radical desorption coefficient for radical A and eq. (48) for radical B for the case where aqueous-phase termination is neglected as is common with conventional relatively water-insoluble monomer systems:

$$k_{\text{des}_A} = K_{oA} \frac{r_A c_{m_{AA}}[M_A]_p + c_{m_{BA}}[M_B]_p}{r_A([M_A]_p + K_{oA}\bar{n}/k_{p_{AA}}) + [M_B]_p} \quad (47)$$

$$k_{\text{des}_B} = K_{oB} \frac{r_B c_{m_{BB}}[M_B]_p + c_{m_{AB}}[M_A]_p}{r_B([M_B]_p + K_{oB}\bar{n}/k_{p_{BB}}) + [M_A]_p} \quad (48)$$

K_{oA} is defined by

$$K_{oA} = 12 D_{wA} \delta'_A / m_{dA} d_p^2 \quad (49)$$

where d_p is the particle diameter, D_{wA} is the diffusion coefficient of monomer A radicals in the aqueous phase, m_{dA} is the partition coefficient for monomer A radicals between the particle and water phases,

$$m_{dA} = \frac{[M_{A^\cdot}]_p}{[M_{A^\cdot}]_w} \quad (50)$$

and δ'_A is the ratio of water-side film mass-transfer resistance to overall mass-transfer resistance for monomer A radicals defined by

$$\delta'_A = \frac{1}{1 + 2D_{wA}/m_{dA}D_{pA}} \quad (51)$$

where D_{p_A} is the diffusion coefficient of monomer A radicals in the polymer particles.

Nomura et al.[10] state that if aqueous-phase termination is not neglected (as in the water-soluble acid–styrene monomer systems), then eqs. (47) and (48) are modified to the form given by

$$k_{\text{des}_A} = \frac{K_{oA}}{\bar{n}} \frac{r_A c_{m_{AA}}[M_A]_p + c_{m_{BA}}[M_B]_p}{r_A([M_A]_p + K_{oA}/k_{p_{AA}}) + [M_B]_p} \quad (52)$$

$$k_{\text{des}_B} = \frac{K_{oA}}{\bar{n}} \frac{r_B c_{m_{BB}}[M_B]_p + c_{m_{AB}}[M_A]_p}{r_B([M_B]_p + K_{oB}/k_{p_{BB}}) + [M_A]_p} \quad (53)$$

An overall average radical desorption coefficient, $\bar{k}_{\text{des}}$ (1/s), is then calculated from

$$\bar{k}_{\text{des}} = \frac{k_{\text{des}_A}}{1 + A} + \frac{k_{\text{des}_B} A}{1 + A} \quad (54)$$

where A is defined by

$$A = \frac{k_{p_{AA}}}{k_{p_{BB}}} \frac{r_B}{r_A} \frac{[M_B]_p}{[M_A]_p} \quad (55)$$

An alternate form of the desorption coefficient, $\bar{k}'_{\text{des}}$ (cm^2/s), which is volume independent, is shown in

$$\bar{k}'_{\text{des}} = V_p^{2/3} \bar{k}_{\text{des}} \quad (56)$$

where V_p is the average swollen particle volume (cm^3). The values of $\bar{k}_{\text{des}}$ (1/s) calculated for the styrene–carboxylic acid systems using the Nomura et al.[10] model are consistent with the trend of values found for other similar monomer systems: styrene 0.02–0.05,[19,12] styrene–methyl acrylate 0.06–1.4,[12] styrene–acrylonitrile 0.2–0.6,[12] and styrene–carboxylic acid 0.1–2.0. The values increase with the overall hydrophilicity of the monomer system.

Mead[12] has developed a model with analytical solutions for predicting the radical desorption coefficient in an emulsion copolymerization system that accounts for nonuniform distribution of free radicals within the particle. Chern[20] has developed a model that accounts for nonuniform distribution of both monomer free radicals and long-chain free radicals inside the particles, but Chern's model requires numerical integration for calculation of the radical desorption coefficient. Results from Mead[12] and Chern[20] reveal that the desorption coefficient increases as the diffusivity in the particle decreases because the free radicals tend to concentrate more at the particle surface than at the particle center when diffusion is slow. Slow diffusion effects are more likely to be prevalent with monomer systems such as the acrylates and methacrylates where the gel effect has been observed to be more significant relative to a styrene or acid–styrene monomer system. The effects of nonuniform radical distributions were not included in this work.

The gel effect was also included in the kinetic model for the acid–styrene systems using a development presented by Sundberg et al.[21] However, the gel effect was determined to be insignificant with the recipes and conditions employed except at very high conversions (> 95%).[22]

Estimation of Radical Entry Rate Coefficients

The average radical entry rate coefficient $\bar{k}_c$ has been estimated for styrene emulsion homopolymerization by several workers with varying results. The mechanism for entry of radicals from the aqueous phase into the polymer particles is complex. The entry rate depends on particle surface effects, which may change over time, rates of radical initiation, rates of diffusion, as well as rates of radical transport from the particles. The mechanism becomes even more complex for copolymerization systems of monomers with different hydrophobicities due to changing copolymer compositions and thus changing hydrophobicities of the oligomeric radicals.

Gilbert et al.[23] and Feeney[24] determine the parameter ρ (1/s), which is the rate of entry as pre-

sented in the classical Smith–Ewart approach. They have developed a method for zero–one systems by which they calculate values of ρ_a and a desorption term, k, from the slope and intercept of batch conversion-time data in the steady-state region where $\rho = \rho_a + \alpha k\bar{n}$. α is shown to be 0 or -1. Given the particle concentration for their system, values of ρ may be converted to $\bar{k}_c$ (cm^3_{aq}/s) by

$$\bar{k}_c = \frac{\rho}{N_p} 1000 \tag{57}$$

where N_p is the particle concentration in numbers of particles/cm^3_{aq}. This calculation results in values between 10^{-18} to 10^{-16} cm^3/s for the styrene homopolymerization system depending on the particle radius, initiator concentration, and number of particles.

Gilbert and Napper's approach is relatively simple for it requires only batch conversion-time data for a series of recipes, and it does not require separate calculations to account for electrostatic repulsion or other particle surface effects. However, it is not easily extended to copolymerizations with water-soluble monomers because of assumptions needed to obtain the slope and intercept of the overall conversion-time curve during the steady-state period. Their results also depend on the nature of the particle surface, which may be much different in an acid–styrene system relative to a styrene homopolymerization system since the acid is hydrophilic and tends to concentrate at the particle surface. A particle surface covered predominantly with carboxyl groups may differ significantly from the surface of particles without carboxylic acid present in the system, and the nature of this surface may change as the copolymer composition changes throughout the course of the reaction.

Hansen and Ugelstad[25] present a more common approach to radical capture in terms of radical diffusion. A system involving irreversible absorption with no electrostatic effects is modeled by

$$\bar{k}_c = 4\pi D_w r \tag{58}$$

where D_w is the diffusivity of monomer in water, and r is the average particle radius.

Since radical desorption and surface effects do exist in most systems, this expression represents an overestimation of the radical capture rate. Therefore, they note that D_w must be modified to account for these phenomena. They report a value of D_w for styrene that leads to a $\bar{k}_c$ of 4×10^{-13} (cm^3/s) for a particle with a diameter of 30–40 nm, which is several orders of magnitude greater than the values obtained from the work of Gilbert and Napper.[23]

Hansen and Ugelstad[25] include a discussion in which they rigorously develop expressions for a reversibility factor (U) and a factor that includes electrostatic effects (W'). This results in the expression for $\bar{k}_c$:

$$\bar{k}_c = 4\pi D_w F r \tag{59}$$

where $F = U/W'$.

A third approach for estimating $\bar{k}_c$ for systems with significant aqueous-phase polymerization rates utilizes steady-state reaction data obtained either from reactions in a continuous stirred-tank reactor (CSTR) or from steady-state portion of the conversion-time curve obtained with most batch data. Continuous reactions were carried out in this work with MAA–styrene and AA–styrene systems using a seed-fed CSTR. Steady-state conversion results from a representative continuous run are presented in Figure 1 for the MAA–styrene system. Steady-state batch reaction rates for styrene were also obtained from the slope of the individual conversion-time curves for styrene for both the MAA–styrene and AA–styrene batch reaction systems at various monomer/water ratios.

The concentrations of the monomers in the particle and aqueous phases were calculated from the partition model using either steady-state conversion

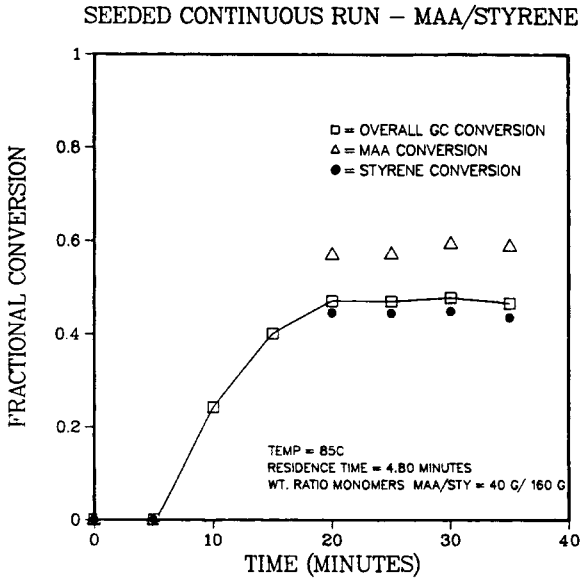

Figure 1 Steady-state conversion-time data for the reaction of MAA–styrene in a CSTR at 85°C with a residence time of 5.1 min (grams acid/grams total monomer = 0.10).

data from the continuous reactions or a selected point along the steady-state portion of the batch conversion curves. A value of $\bar{n}$ was obtained by assuming that the rate of reaction of styrene in the aqueous phase is negligible compared to the rate in the particles. The steady-state rate of reaction of each monomer can be determined from individual monomer conversion measurements. If the reaction of styrene is assumed to take place primarily in the particles, $\bar{n}$ may be calculated directly using

$$\bar{n} = \frac{R_{pB} N_A}{(N_p)\left(k_{p_{BB}} \frac{A}{1+A} + k_{p_{AB}} \frac{1}{1+A}\right)[B]_p} \tag{60}$$

where

$$A = \frac{k_{p_{AA}}}{k_{p_{BB}}} \frac{r_B}{r_A} \frac{[B]_p}{[A]_p}$$

$\bar{k}_{\text{des}}$ may be estimated using equations developed by Nomura et al.[10]

Ugelstad and Hansen[11] present a method for calculating $\bar{n}$ that accounts for reabsorption of radicals into the particles and aqueous-phase termination. A mass balance on the aqueous-phase free radicals for a batch system is given by

$[R_c$ = rate of capture (mol/L_{aq} s)].

R_c = rate of formation + rate of desorption − rate of termination

$$R_c = \frac{\bar{k}_c N_p [R_{\text{tot}}]_{\text{aq}}}{1000} = 2 f k_d [I] + \bar{k}_{\text{des}} \bar{n} N_p / N_A + 2\bar{k}_{tw} [R_{\text{tot}_{\text{aq}}}]^2 \tag{61}$$

This expression may be rewritten in terms of dimensionless variables as described by

$$\alpha_n = \alpha'_n + m\bar{n} - Y\alpha_n^2 \tag{62}$$

where

$$\alpha_n = \frac{R_c N_A^2 (V_p / V_{\text{aq}})}{k_{tp} N_p^2} \tag{63}$$

$$\alpha'_n = \frac{R_i N_A^2 (V_p / V_{\text{aq}})}{k_{tp} N_p^2} \tag{64}$$

$$m = \frac{k_{\text{des}} (V_p / V_{\text{aq}}) N_A}{N_p k_{tp}} \tag{65}$$

$$Y = \frac{2 k_{tw} k_{tp} N_p^2}{N_A^2 \bar{k}_a^2 (V_p / V_{\text{aq}})} \tag{66}$$

$\bar{n}$ may then be calculated from Bessel functions as given by

$$\bar{n} = \frac{a}{4} \frac{I_m(a)}{I_{m-1}(a)} \tag{67}$$

where $a = \sqrt{8\alpha_n}$. The Bessel functions may be solved by the method of continued fractions described by Ugelstad and Hansen.[11] All parameters in eqs. (63)–(66) are known from the reaction conditions or can be calculated using appropriate correlations except for the absorption coefficient, $\bar{k}_a$ (1/s), which may be expressed as a function of the average capture coefficient, $\bar{k}_c$ (cm^3/s) by

$$\bar{k}_a = \frac{\bar{k}_c N_p}{1000} \tag{68}$$

Using the calculated value of $\bar{k}_{\text{des}}$ obtained with the Nomura et al. model,[10] $\bar{k}_c$ may then be adjusted until the calculated $\bar{n}$ matches the experimental value. This procedure is useful only in the range where the parameter Y is large (> 100) since $\bar{n}$ is not very sensitive to changes in Y, and thus $\bar{k}_c$, when Y is small. Due to the large number of particles (N_p) and small particle size (diameter $\approx$ 30–40 nm), reasonably large values of Y ($\sim$ 100–900) were obtained under the reaction conditions employed in this work.

Both steady-state continuous reaction and batch reaction data were investigated. However, the results reported in this work are based primarily on data obtained from the steady-state region of batch conversion-time curves for both MAA–styrene and AA–styrene systems since reactions in CSTRs result in rather broad particle size distributions. Batch reactions only exhibit steady-state reaction rates over a limited reaction period. However, the particles in batch reactions are often monodisperse, which minimizes the effects of different particle sizes on the average rate of capture.

The dependence of $\bar{n}$ on the average capture coefficient for various values of $\bar{k}_{\text{des}}$ under the conditions of the reactions used in this study is shown in Figures 2 and 3 for the MAA–styrene and AA–styrene systems, respectively. $\bar{n}$ increases as $\bar{k}_c$ increases initially. When $\bar{k}_c$ continues to increase, the parameter Y approaches zero, and further changes in $\bar{k}_c$, and thus Y, have little effect on $\bar{n}$. The value of $\bar{n}$ for any given $\bar{k}_c$ depends also on the rate of desorption represented by $\bar{k}_{\text{des}}$.

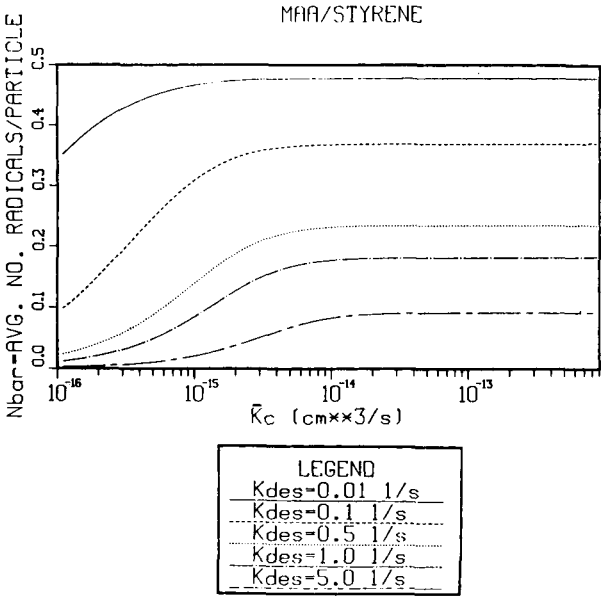

Figure 2 Dependence of $\bar{n}$ on the average capture coefficient at various values of $\bar{k}_{des}$ for the MAA–styrene system at an α'_n of 2.0×10^{-5}.

The dependence of the aqueous-phase free-radical concentration and the parameter Y on $\bar{k}_c$ for each system are shown in Figures 4, 5, and 6. The aqueous-phase free-radical concentration, $[R_{tot}]_{aq}$, decreases with both $\bar{k}_c$ and $\bar{k}_{des}$, as expected. The value of Y is greater for the AA–styrene system than for the MAA–styrene system due to the higher rate of termination of AA than MAA.

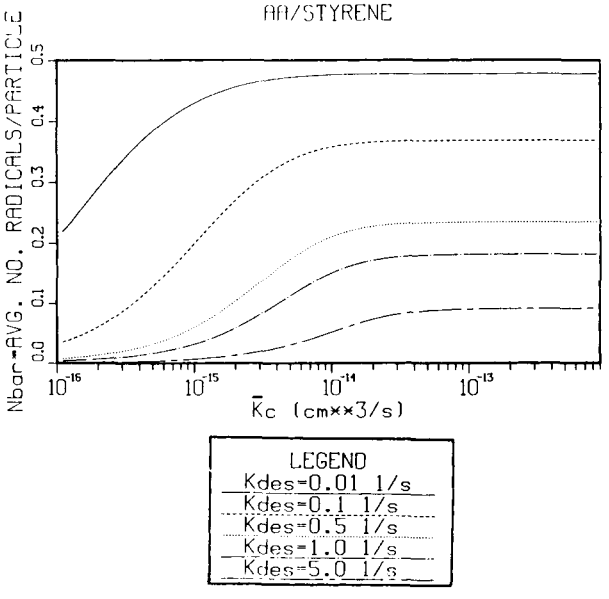

Figure 3 Dependence of $\bar{n}$ on the average capture coefficient at various values of $\bar{k}_{des}$ for the AA–styrene system at an α'_n of 1.7×10^{-5}.

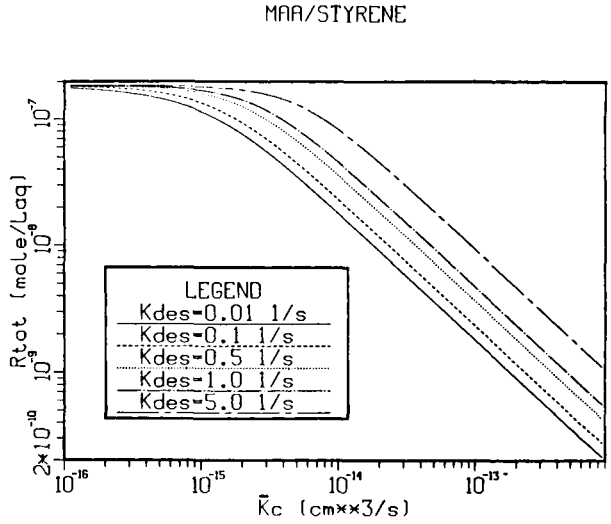

Figure 4 Dependence of the aqueous-phase free-radical concentration on the average capture coefficient at various values of $\bar{k}_{des}$ for the MAA–styrene system at an α'_n of 2.0×10^{-5}.

Mead[12] used an approach for the MA–styrene system similar to the steady-state continuous reaction approach described earlier except he utilized particle size distribution data instead of reaction rate data, and he fit the parameter W defined by Ugelstad. His simulations resulted in $\bar{k}_c$ values ranging between 2×10^{-17} and 2×10^{-15} cm^3/s. Analysis of the experimental data from the studies of the MAA–styrene and AA–styrene systems as discussed previously resulted in $\bar{k}_c$ values ranging between 7

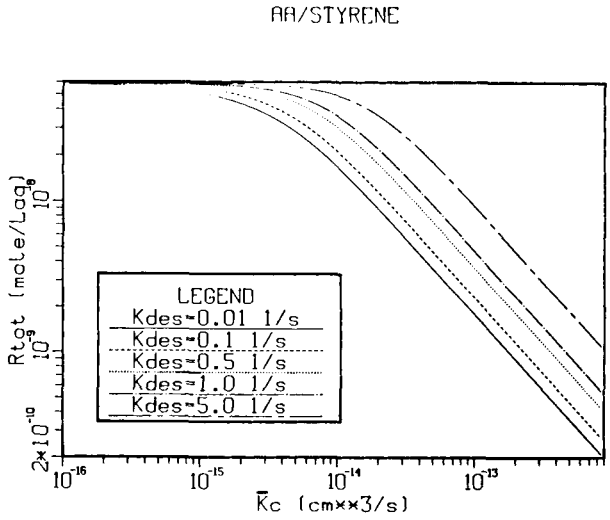

Figure 5 Dependence of the aqueous-phase free-radical concentration on the average capture coefficient at various values of $\bar{k}_{des}$ for the AA–styrene system at an α'_n of 1.7 $\times 10^{-5}$.

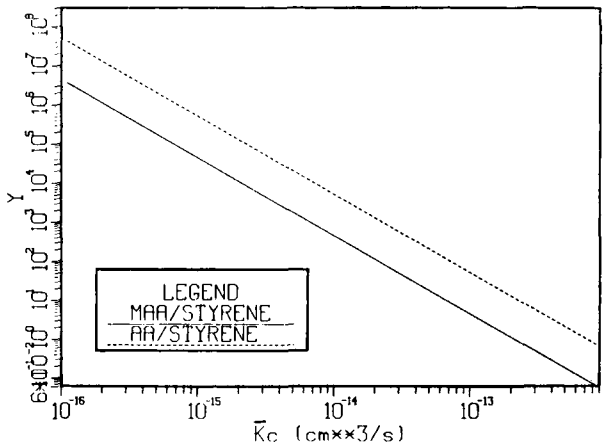

Figure 6 Dependence of dimensionless parameter Y on the average capture coefficient at various values of $\bar{k}_{des}$ for the MAA–styrene (α'_n of 2.0×10^{-5}) and AA–styrene systems (α'_n of 1.7×10^{-5}).

$\times 10^{-15}$ and 7×10^{-14} cm^3/s. A summary of the reported values for the various systems is shown in Table II.

It is apparent that there is a great deal of discrepancy in the values of $\bar{k}_c$ reported. Values of $\bar{k}_c$ obtained for the acid–styrene systems are larger than values obtained for the MA–styrene system, which in turn are also larger than the range reported by Gilbert and Napper[23] and Feeney[24] for the styrene homopolymerization system. It is unclear why the capture rate constant tends to increase when a more hydrophilic monomer is added to the system. However, one factor that may contribute to the increased capture rates is that the propagation constants also increase in the same order as the hydrophilicity for these monomers (styrene < MA < MAA < AA). A faster propagation reaction would increase the rate of growth of an oligomer radical to the critical chain length at which capture is most likely to occur. Evidence of this phenomenon is obtained from results reported by Hawkett et al.[26] where they show qualitatively that the capture efficiency for more water-soluble monomers (methyl methacrylate, vinyl acetate, vinyl chloride, and acrylonitrile) is higher than that for styrene due to their faster rates of propagation to reach the critical chain length required for capture to occur. An opposing factor to increased rate of capture is the fact that a more hydrophilic monomer will require a greater critical chain length before it becomes "hydrophobic" enough to make capture likely. However, the results from these acid–styrene studies as well as the MA–styrene system imply that the effect of an increased rate of propagation to the critical chain length needed for capture is greater than the effect of having to grow to a longer chain length before becoming hydrophobic enough to be captured when compared to results from the styrene studies (with the exception for the value of $\bar{k}_c$ obtained for styrene based on Hansen and Ugelstad's[25] results).

An additional factor that may have large effects on the rate of capture is the nature of the particle surface. Both steric and electrostatic effects play an important role in determining how easily an oligomer radical will penetrate through the surface of the particle. Therefore, addition of other components that may contribute to surface effects such as surfactant or initiator should be considered before applying reported values for capture coefficients to a particular reaction system. In addition, the character of the surface may change over the reaction period in copolymerization systems, especially when monomers such as itaconic acid, AA or MAA are utilized. These monomers tend to concentrate at the particle surface due to their hydrophilic nature. Therefore, a styrene seed particle with a hydrophobic surface may eventually become coated by the hydrophilic monomer as the reaction proceeds. This coating may significantly change the character of the particle surface, which in turn may affect the rate at which oligomeric radicals diffuse from the aqueous phase to the particle interior.

The estimates of $\bar{k}_c$ reported in this work for the MAA–styrene and AA–styrene systems were obtained with a relatively simple experimental approach. This approach may be applied to many similar monomer systems in order to obtain order-of-magnitude estimates for the average capture coefficients under a given set of reaction conditions. The resulting values, however, depend on the accuracy of the experimental data as well as the accuracy of the parameters utilized in the copolymerization rate equations for calculating $\bar{n}$ and $\bar{k}_{des}$, and they do not reflect potential effects from the changing nature of the particle surface throughout the reaction period. Therefore, more rigorous approaches for determin-

Table II Reported Values of Capture Coefficients for Several Monomer Systems

Source	System	$\bar{k}_c$ (cm^3/s)
23	Styrene	10^{-18}–10^{-16}
12	MA–styrene	2×10^{-17}–2×10^{-15}
This work	MAA–styrene	7×10^{-15}–7×10^{-14}
	AA–styrene	—
25	Styrene	3×10^{-13}

ing $\bar{k}_c$ for copolymer systems with water-soluble monomers are needed.

Nevertheless, the general approach used in this study appears to give reasonable estimates for $\bar{k}_c$. The average values obtained for the acid–styrene systems correspond to the trend of increasing $\bar{k}_c$ with increasing propagation rate (and increasing hydrophilicity) exhibited by other monomer systems, and when used in the batch copolymerization model, these same values result in the best fits of the experimental batch copolymerization data. Values of $\bar{k}_c$ in the range reported by Mead[12] and Gilbert and Napper[23] are too small to provide reasonable fits of conversion-time data for the MAA–styrene and AA–styrene systems, unless unreasonably low values for $\bar{k}_{des}$ are used in the copolymerization model.

EXPERIMENTAL

Acrylic acid, methacrylic acid, and styrene monomer (all > 90% pure) were used as received. Potassium persulfate and sodium dodecyl sulfate were also used as received. Carboxylated styrene seed particles (28 nm diameter) were supplied by Dow Chemical, Midland, Michigan. High-purity nitrogen (> 99%) was employed.

All of the batch reactions utilized monomers that contained a small amount of inhibitor added by the manufacturer to prevent polymerization during shipping. Removal of inhibitor is unnecessary for most batch runs since the only effect in most cases is the occurrence of an induction period at the beginning of the reaction during which the inhibitor is consumed. The reaction then proceeds in normal fashion. (Due to the low levels of inhibitor in the monomers and the high reaction temperatures, no induction period was observed for the reactions performed in this study.) This assumption was checked by performing a MAA–styrene run using "cleaned" monomers and comparing the results to runs made with "uncleaned" monomers. Styrene was cleaned for this run by washing with 5.0 wt % KOH solution followed by filtration through an alumina packing, and the MAA was distilled under vacuum. No difference was observed in the conversion-time behaviors.

The standard recipe for each of the seeded emulsion copolymerization reactions is given in Table III.

All emulsion polymerization reactions were run at 85°C in a nitrogen-purged, agitated, 1.0-L glass vessel similar to the reactor used for the solution polymerizations. The following procedure was used for each run. Carboxylated, styrene seed latex was mixed for 24–48 h with an anionic–cationic ion exchange resin (Bio-Rex MSZ 501) in order to remove excess surfactant. The amount of surfactant removed from the seed was determined gravimetrically. Deionized water, "cleaned" seed, and SDS (an amount combined with the SDS remaining in the seed latex to give a concentration of 4.0 mmol/L_{aq}) was added to the reactor. Nitrogen was bubbled into the reactor and heating was begun by pumping hot water through an internal stainless-steel coil. When the reactor temperature reached approximately 85°C, styrene was slowly added through a dropping funnel. The acid monomer was then slowly added in the same manner. Fast addition of either monomer would tend to "shock" the seed, resulting in coagulation. The nitrogen purge line was pulled to the top level of the emulsion after the monomer addition to prevent polymer from coagulating at the interface of the nitrogen bubbles.

Samples of 20–25 mL were extracted with a syringe, immediately injected into a chilled hydroquinone solution, and immersed in an ice bath to quench the reaction. The overall conversion was measured gravimetrically by drying about 5 g of each sample overnight in an oven and performing a mass balance on the dried solids.

Individual monomer conversions were obtained by gas chromatography (GC) using a Varian 3300 with a 12-ft stainless-steel column packed with Gas

Table III Standard Recipe for Carboxylated Emulsion Batch Copolymerizations

$K_2S_2O_8$	5.0 mmol/L_{aq}
Sodium dodecyl sulfate (SDS)	4.0 mmol/L_{aq} (CMC = 9.0 mmol/L_{aq})
Seed (particle diameter ~ 28 nm)	~ 30 g of solid polymer ~ 4.0×10^{18} particles/L_{aq}
Monomer	200 g total
Acid–styrene ratios	0/200, 20/180, 40/160, 70/130
DI water	Balance to give 1000 g total reaction mass

Chrom 254, 80–100 mesh packing. (The packed column was supplied by Alltech Associates in Deerfield, Illinois.) The column was operated at 220°C, and an internal standard was used in each sample.

Seeded continuous reactions were run in a 0.25-L glass, jacketed continuous stirred-tank reactor (CSTR). "Cleaned" monomers were used for all continuous runs. Monomer, water, and cleaned seed were preemulsified, purged with nitrogen, held in a glass vessel with constant stirring. Potassium persulfate was dissolved in water, purged, and stored in a second glass vessel. The mixtures were pumped separately into the CSTR using calibrated peristaltic pumps. The CSTR was heated by a hot water–ethylene glycol mixture that was pumped through the external jacket. A thermocouple, digital temperature controller, and water–ethylene glycol bath as already described were utilized to maintain a constant reaction temperature. Samples were collected from the overflow of the reactor at various time intervals and the conversion was measured using both GC and gravimetric analysis.

RESULTS AND DISCUSSION

Seeded Styrene Homopolymerization

Seeded reactions with styrene alone were initially performed at 85°C using the standard recipe shown in Table II. Unseeded homopolymerization reactions of styrene often require several hours to reach high conversion. However, the use of seed particles can cause the reaction to occur much more quickly as observed with the experimental conversion data shown in Figure 7. The primary reason for using seeded reactions was to avoid particle nucleation so that the study could be more easily focused on the reaction kinetics.

The seeded styrene homopolymerization was modeled with the basic emulsion polymerization reaction rate equation.

$$R_p = k_p[M]_p \bar{n} \frac{N_p}{N_A} \tag{69}$$

A k_p value of 900 L/mol s was used for the propagation constant for styrene at 85°C.[27] This value was determined from an Arrhenius-type plot based on experimental k_p values for styrene obtained over a large range of temperatures by a variety of different workers. The amount of swelling of the particles was based on work with styrene polymerization systems performed by Jannson.[28] Results of this work suggested that the volume ratio of monomer to polymer in the particles should be $\approx$ 1.5 during interval II based on the average particle sizes. Interval III was assumed to begin when the total volume of monomer in the system became less than 1.5 times the volume of polymer. All of the styrene was then assumed to be inside the particles. The average number of radicals per particle, $\bar{n}$, was varied from 0.1 to 0.4. A value of $\bar{n}$ of 0.30 gives the best overall fit to the experimental data as revealed in Figure 7. However, $\bar{n}$ will vary with conversion. Therefore, in the emulsion copolymerization model $\bar{n}$ is calculated separately throughout the conversion period using the method developed by Ugelstad and Hansen[11] referred to earlier.

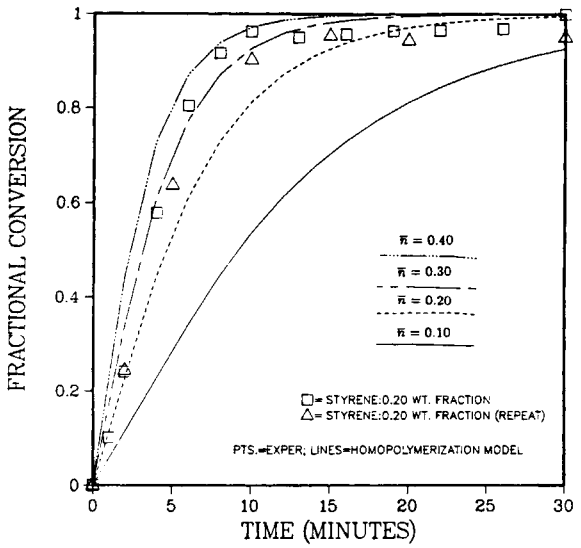

Figure 7 Experimental and predicted conversion-time data for a seeded emulsion homopolymerization of styrene.

Seeded Emulsion Copolymerization of MAA–Styrene and AA–Styrene Systems

Batch seeded emulsion copolymerization reactions of MAA–styrene and AA–styrene were run at 85°C using the standard recipe given in Table III. Conversion-time measurements were made using gas chromatography and gravimetric analyses. Three weight ratios of acid/styrene were used: 20/180, 40/160, and 70/130. Conversion-time results for the 40/160 acid/styrene weight ratios along with the model predictions are shown in Figures 8 and 9 for the MAA–styrene and AA–styrene systems, respectively.

The reactions with the acids are rapid, with nearly complete conversion attained in about 10–20 min. However, these reactions are somewhat slower than

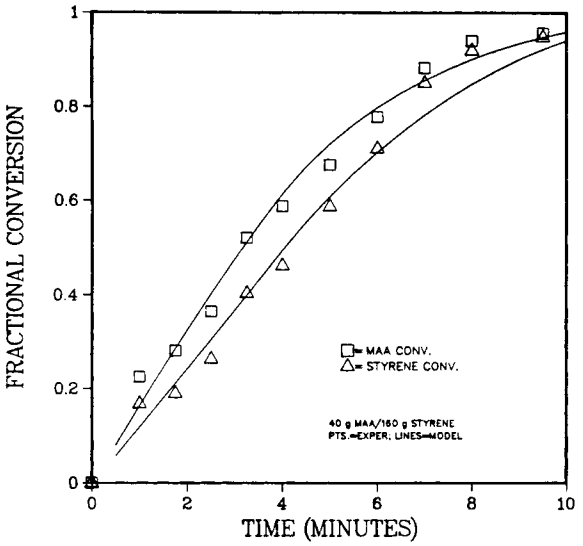

Figure 8 Comparison of predicted and experimental conversion-time data for the seeded batch emulsion copolymerization of MAA–styrene at a weight ratio of 40 g MAA/160 g styrene using a variable value of $\bar{k}_{des}$.

the homopolymerization of styrene under the same reaction conditions and particle concentrations. MAA reacts more quickly than does AA despite the fact that its propagation constant is less than that of AA. One reason for the faster rate with MAA is attributed to the fact that it is more hydrophobic than AA so that it distributes to a greater extent inside the particles where the monomer and free-radical concentrations are generally higher. MAA conversion becomes high at about the same time as styrene. However, for the same ratios of acid–styrene, the AA conversion significantly lags that of styrene. A substantial portion of AA does not react until most of the styrene monomer has been depleted. The primary reaction locus in the AA–styrene reaction may actually shift from the particles to the aqueous phase after the styrene has been depleted from the system. Additional experiments designed for more thorough investigation of the reaction mechanism for the AA–styrene system will be discussed later.

Model Assumptions for Seeded Batch Copolymerizations of MAA–Styrene and AA–Styrene Emulsion Systems

Simulations of seeded batch emulsion copolymerizations of MAA–styrene and AA–styrene systems were conducted with the model equations developed in the previous sections. Assumptions and conditions used in the model are as follows.

1. The reaction system is seeded and the particle number remains constant. Any new particles formed due to homogeneous nucleation flocculate onto preexisting particles due to the large particle concentration ($\approx 4.0 \times 10^{18}$ particles/L_{aq}) in the system.
2. All aqueous-phase polymer flocculates onto the polymer particles. Because a relatively small amount of overall polymer is formed in the aqueous phase, this assumption has little effect on the predicted conversion-time behavior. Calculations based on the assumption that all of the aqueous-phase polymer remains in the aqueous phase gives almost identical results.
3. The average number of radicals per particle, $\bar{n}$, was calculated from a relation developed by Ugelstad and Hansen[11] as discussed in the previous section.
4. The average radical capture constant, $\bar{k}_c$, was determined from separate batch and continuous reaction studies and was assumed constant throughout the reaction period.
5. The desorption constant, $\bar{k}_{des}$, varied with monomer concentrations in the aqueous and particle phases, and it was calculated using a model proposed by Nomura et al.[10] as modified to account for aqueous-phase polymerization.

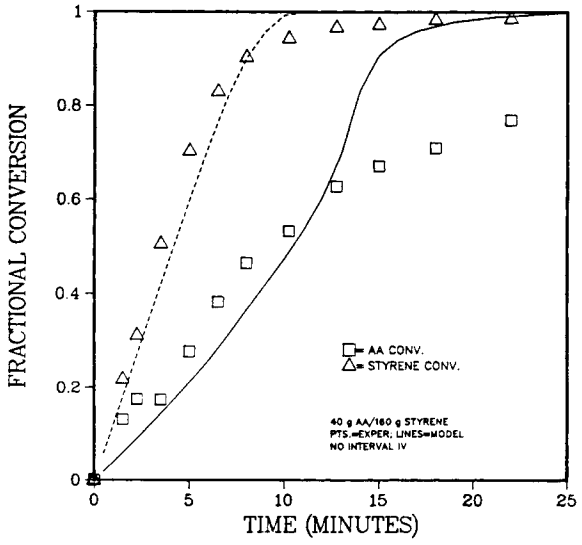

Figure 9 Experimental (points) and predicted (line) conversion-time data for the AA/styrene (40/160 g) seeded emulsion copolymerization system at 85°C. The model assumes that reaction occurs in both the particle and aqueous phases throughout the conversion period (i.e., no interval IV).

6. Values for diffusivities in water of each monomer were calculated using the Wilke–Chang correlation.[34] Values for the diffusivities in the polymer particles were assumed to be approximately 0.1 times the diffusivity in water.[12,19]
7. Values of chain transfer constants in the range reported for methyl acrylate (0.01×10^{-4} to 0.4×10^{-4},[27]) were used for MAA and AA. Values for chain transfer constants ($c_{m_{ii}}$) for the MAA and AA are not available in the literature. However, the structure of MAA and AA are similar to that of methyl acrylate (MA) as shown in Figure 10. Therefore, values for chain transfer constants used in the model for MAA and AA were chosen within the range reported for MA in the literature. Values used in the model for styrene were, likewise, restricted to the range reported for styrene in the literature (0.5×10^{-4} to 1.8×10^{-4}).[27]
8. Values for cross-chain transfer constants were assumed to be 0.1 times the chain transfer constants for each monomer (i.e., $c_{m_{AB}} = 1/10\ c_{m_{BB}}$ and $c_{m_{BA}} = 1/10\ c_{m_{AA}}$). Values of cross-chain transfer constants ($c_{m_{ij}}$) are also not available in the literature. Since the difference in hydrophobicity between styrene and MAA or AA is so large, these monomers are not likely to associate with each other as much as with "like" monomer molecules. The cross-chain transfer between the acid–styrene molecules is probably much lower than between acid–acid or styrene–styrene molecules. The model results were not very sensitive to the selection of $c_{m_{ij}}$. Therefore, this assumption is not very critical.

CHEMICAL STRUCTURES

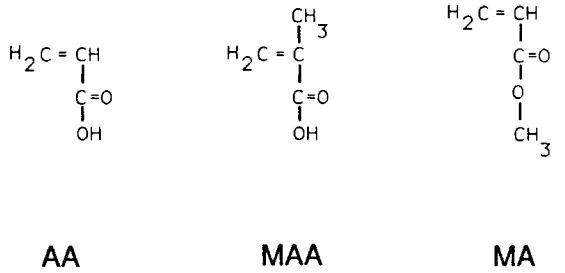

Figure 10 Chemical structure of AA, MAA, and MA monomers.

9. The concentration of styrene monomer in the aqueous phase was based on values reported by Brown and Taylor[35] that were dependent on the concentration of acid in the aqueous phase. (Due to the low concentration of styrene in the aqueous phase and its subsequent small effect on the mass balances in the partition model, it was difficult to obtain accurate predictions of the aqueous-phase concentration of styrene from the partition model. Therefore, more accurate values obtained from the literature were used in the simulations in order to obtain accurate predictions of desorption constants without significantly affecting the overall mass balances calculated by the partition model).

Partition of the monomers between the aqueous, particle, and droplet phases is predicted through a combination of mass balances and thermodynamic free-energy relations that depend on the volume of each phase, the volume of monomer, and interaction between the monomers, polymer particles, monomer droplets, and aqueous phase. Interaction parameters employed in the thermodynamic equations were obtained from separate independent experiments. Details of these monomer partition calculations are presented by Shoaf [22] and Shoaf and Poehlein.[36]

Values for the various parameters used in the kinetic model are listed in Table IV.

The chain transfer constant, $c_{M_{AA}}$, used for AA was smaller than that used for MAA (4). The chain transfer constant is defined by eq. (70), which relates the rate of chain transfer to the rate of propagation for a given monomer:

$$c_{M_{ij}} = k_{tr}/k_{p_{ii}} \tag{70}$$

Litt[37] suggests that radical transfer for the vinyl acetate monomer is to the vinyl group, and Mead,[12] by analogy, states that the vinyl group of MA may also provide a stable site for chain transfer. Except for the carboxyl group, the structures of MAA and AA are similar to MA, which again suggests that the most likely site for chain transfer is the vinyl group. However, the extra methyl group on the vinyl carbon with MAA helps to stabilize a free radical more than the hydrogen atom on the AA molecule. Therefore, MAA is more likely to release a hydrogen and stabilize the resulting radical species than AA, which maintains a stronger hold on the vinyl hydrogens. This fact suggests that k_{tr} should be greater for MAA than for AA. In addition, the propagation constant, k_p, is significantly greater for AA than for

Table IV Values for Parameters Used in Seeded Emulsion Copolymerization Simulation (T = 85°C)

Parameter	Monomer	Value	Source
k_p (L/mol s)	MAA	15,900	Experiment, 29
	AA	76,900	Experiment, 29
	Styrene	900	27
k_t (L/mol s)	MAA	0.1×10^8	30, 31
$k_{tw} = k_{tp} = k_t$	AA	1.0×10^8	30, 31
	Styrene	2.5×10^8	27
r_A	MAA	0.55	32, 33
r_B	Styrene	0.25	32, 33
r_A	AA	0.1	32, 33
r_B	Styrene	0.9	32, 33
$c_{m_{AA}}$	MAA	0.25×10^{-1}	27
$c_{m_{AA}}$	AA	0.25×10^{-5}	27
$c_{m_{BB}}$	Styrene	$0.5\text{–}1.0 \times 10^{-4}$	27
$\bar{k}_c$ (cm^3/s)	MAA/Sty	2.0×10^{-14}	This work
	AA/Sty	7.0×10^{-14}	This work
N_p (part/$L_{reactor}$)	3.0×10^{18}	$\approx 4.0 \times 10^{18}$ (part/L_{aq})	

MAA. These results suggest that the chain transfer constant, $c_{m_{AA}}$, should be smaller for AA than for MAA. Results of the model simulations revealed that better fits of the experimental data were obtained when the value of $c_{m_{AA}}$ for AA was smaller than that for MAA. Therefore, the values used in the model were selected within the range reported for methyl acrylate, but a somewhat lower value was used for AA than for MAA (Table IV).

MAA–Styrene: Conversion Profiles and Reaction Rates

The overall model for the MAA–styrene system is shown to predict the experimental data quite well for a range of monomer concentrations using no adjustable parameters as shown in Figures 8, 11, and 12 for the 20/180, 40/160, and 70/130 MAA/styrene ratios, respectively. Good fits of the conversion-time behavior for both MAA and styrene are obtained over the full range of conversion. Typical model predictions of the rates of reaction of styrene in the particle phase and MAA in both particle and aqueous phases for the 40/160 recipe are shown in Figure 13. The aqueous-phase polymerization rate of MAA is less than the polymer-phase polymerization rate by more than an order of magnitude for all three monomer ratios. However, it is still significant, especially when considering the effects that small amounts of acids have on product properties. The aqueous-phase polymerization rate of styrene is several orders of magnitude less than the aqueous-phase polymerization rate of MAA, and it is not shown in Figure 13. Prediction of other important parameters such as $\bar{n}$, $\bar{k}_{des}$, R_{tot}, particle diameter, and copolymer compositions are discussed in detail by Shoaf.[22]

AA–Styrene: Conversion Profiles and Reaction Rates

Typical model results for the AA–styrene system are presented in Figure 9. A reasonable fit of the 40/160 experimental data is obtained until the sty-

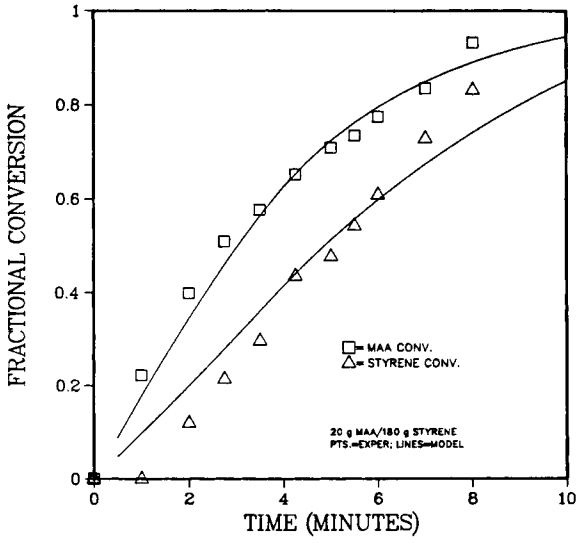

Figure 11 Comparison of predicted and experimental conversion-time data for the seeded batch emulsion copolymerization of MAA/styrene at a weight ratio of 20 g MAA/180 g styrene using a variable value of $\bar{k}_{des}$.

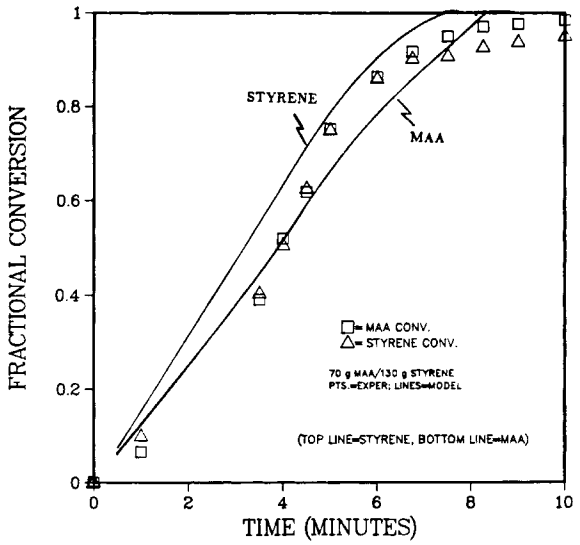

Figure 12 Comparison of predicted and experimental conversion-time data for the seeded batch emulsion copolymerization of MAA/styrene at a weight ratio of 70 g MAA/130 g styrene using a variable value of $\bar{k}_{des}$.

rene disappears. The model at this point overestimates the reaction rate of AA. The model predicts that the AA reaction in the particles accelerates once the styrene is depleted due primarily to the large propagation constant of the AA radicals with AA monomer (76,900 L/mol s) relative to the cross-propagation constant for styrene radicals with AA monomer ($k_{p_{BA}}$ = 1000 L/mol s). The experimental reaction rate of AA does not accelerate after styrene has reached high conversions.

AA is very hydrophilic and does not partition to a large extent into the particles. The slow reaction rate of AA relative to the model predictions observed after styrene has been depleted is more representative of the reaction rate expected in the aqueous phase where the monomer and free-radical concentrations are usually lower than in the particles. Determining the primary reaction locus during this phase of the reaction may be important for understanding the mechanism for the seeded AA–styrene reaction, especially after the styrene has been consumed.

Interval IV in Emulsion Copolymerization

The reaction locus in most conventional emulsion systems is almost exclusively inside the polymer particles. Systems that contain both a hydrophobic and a hydrophilic monomer may exhibit reaction in both the aqueous and particle phases. (Some reaction may also occur in the monomer droplets. However, due to the small number of droplets relative to the number of polymer particles, reaction in the droplet phase is usually negligible, except in miniemulsions.) Kawaguchi[38] showed that with the styrene–acrylamide system, the reaction locus actually started in the aqueous phase (where almost 99% of the acrylamide was located), moved to the polymer particles as styrene became incorporated into the oligomeric radicals, then moved back into the aqueous phase after the styrene was depleted.

The AA–styrene system is very similar to the acrylamide–styrene system except that a larger amount of AA partitions into the particles than does acrylamide. The reaction locus in the AA–styrene system is probably located in both the aqueous and particle phases initially, but there is evidence to suggest that the locus shifts back into the aqueous phase after the styrene is depleted. The seeded copolymerization model predicts the styrene conversion fairly well to high conversions as shown in Figure 9. However, the model predictions for AA conversion diverge from the experimental values after the styrene has been depleted. This result suggests that the reaction locus may shift back into the aqueous phase once the concentration of styrene in the system becomes very low.

If the aqueous phase is not saturated with styrene monomer, the oligomers would be very hydrophilic and thus unlikely to diffuse into the polymer particles. Also since polyAA tends to build up on the surface of the particles based on numerous titration studies reported in the literature,[2,5,7] the particles may possess a coating of hydrophilic polyAA that

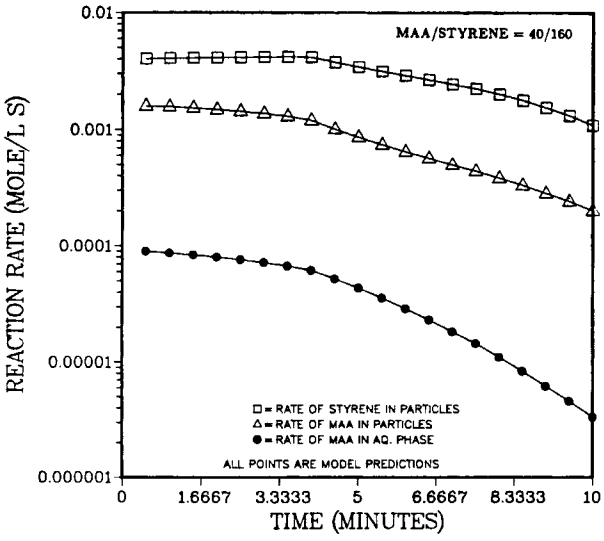

Figure 13 Predicted reaction rates of MAA and styrene as a function of time for an acid/styrene ratio of 40/160.

would tend to trap hydrophilic oligomer radicals, thus preventing their penetration into the polymer particles. The reaction would then occur exclusively in the aqueous phase. The point near the end of the reaction where the reaction locus shifts to the aqueous phase will be referred to as interval IV. Figure 14 provides a physical description of the system during interval IV.

One assumption made in the preceding analysis is that reaction of AA in the particles should be faster than reaction of AA in the aqueous phase. To test this assumption, styrene was removed from the system and a seeded homopolymerization of AA was conducted using the same initiator and initial monomer concentrations as used in a previous unseeded solution polymerization of AA. The resulting data was modeled assuming (i) only aqueous-phase polymerization and (ii) both aqueous-phase and particle-phase polymerization. A reasonable fit of the data was obtained for case (i) with f_{eff} set to 0.35 as shown in Figure 15. (The model for this case was analogous to an emulsion homopolymerization model. It included effects of monomer partitioning, radical capture, and desorption by the particles. Thus it was not limited to the simple solution polymerization case.) When particle-phase polymerization was also included in the model, the predicted reaction rate was much greater than that observed unless the average number of radicals per particle was set to very low values, less then 0.0005. (See Fig. 16.) Therefore, if significant AA reactions were taking place in the particle phase, the model predicts that the reaction rate would be much higher than the rate observed.

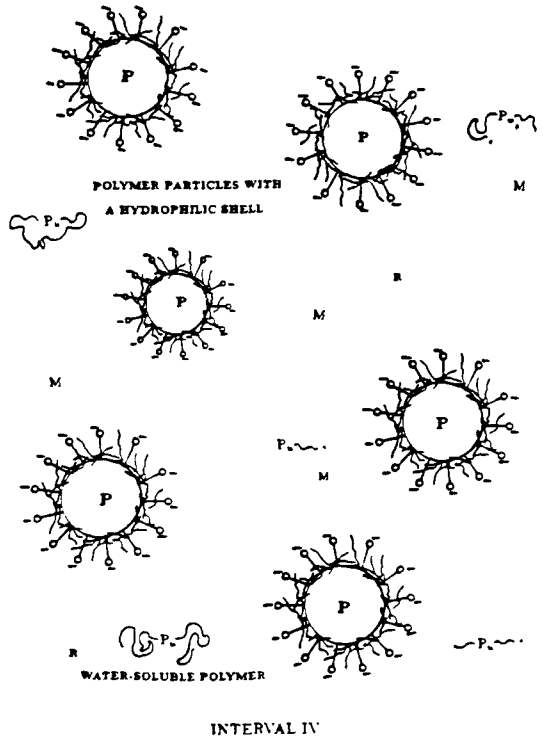

Figure 14 Emulsion copolymerization system during interval IV (P = polymer; M = monomer; R = free radical).

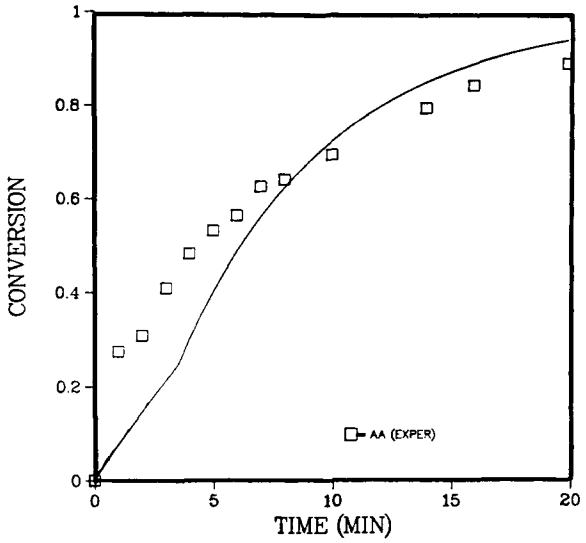

Figure 15 Model simulation of seeded homopolymerization of AA assuming only aqueous-phase polymerization. Particle number = $4 \times 10^{18}/L_{aq}$, $f_{eff} = 0.35$.

When the seeded homopolymerization data for AA was plotted along with the unseeded homo-

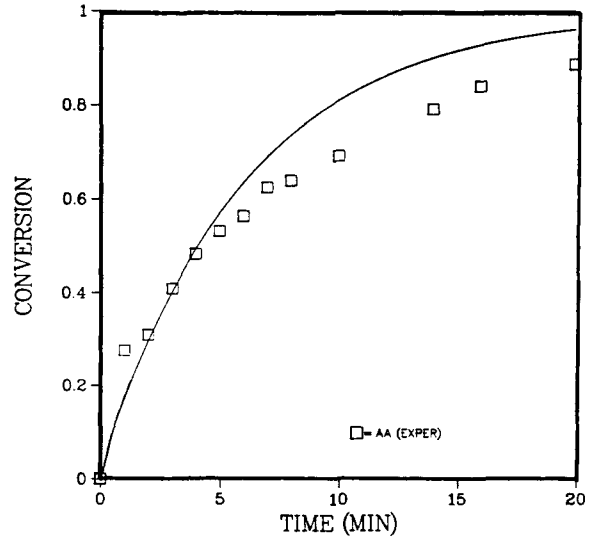

Figure 16 Model simulation of seeded homopolymerization of AA assuming both aqueous-phase and particle-phase reactions (particle number = $4 \times 10^{18}/L_{aq}$, $f_{eff} = 0.35$, and $\bar{n} = 0.0005$).

polymerization data (Fig. 17), the curves were almost identical. This result suggests that without the presence of styrene, the AA oligomer radicals do not penetrate the particles and initiate reaction in the particle phase.

A semibatch run of AA–styrene was performed to further test this conclusion. The precept was that if part of the styrene is fed to the reactor later in the reaction period, the styrene should help pull the oligomer radicals into the particles and thus increase the polymerization rate of AA relative to the case where essentially all of the styrene in the system has been depleted. Thirty-five percent of the styrene was fed over a 17-min period starting at 6 min into the reaction. All of the AA was added at the beginning of the reaction. Figure 18 shows the styrene concentration profiles for the batch and semibatch runs. The data show that a significant concentration of styrene was present in the reactor over the continuous addition period as desired. The AA concentration profiles, however, for both the batch and semibatch runs were almost identical as revealed in Figure 19. (Monomer concentrations were based on the final volume of the reaction contents for these runs.) The AA did not tend to react faster at higher conversions when in the presence of styrene as first expected.

The initial conclusion is that the styrene was unable to pull the radicals into the particles where both AA and styrene should react. However, since the styrene concentration does not build up during the continuous feed period, it must have reacted, and this reaction inevitably takes place inside the particles along with the AA monomer. However, the AA reaction rate does not show an increase.

A closer look at the reaction rate equations reveals that the presence of a significant amount of styrene in the particles may prevent the AA reaction rate from rising as expected in the semibatch case. This result can be obtained by calculating parameter A,

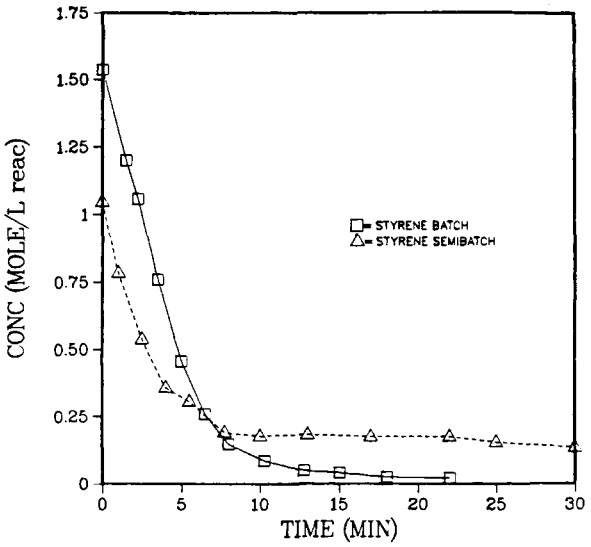

Figure 18 Styrene concentration for a batch and semibatch AA/styrene (40/160 g) seeded copolymerization. Thirty-five percent of the total styrene was fed continuously over a 17-min period starting at 6 min.

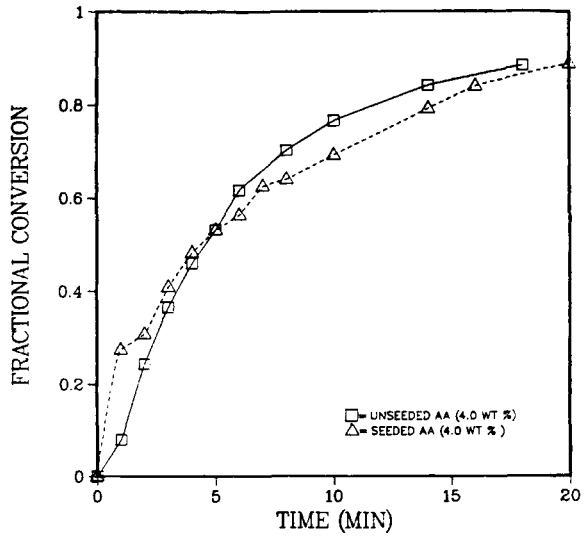

Figure 17 Comparison of conversion-time data for the homopolymerization of AA in a seeded and unseeded reaction system.

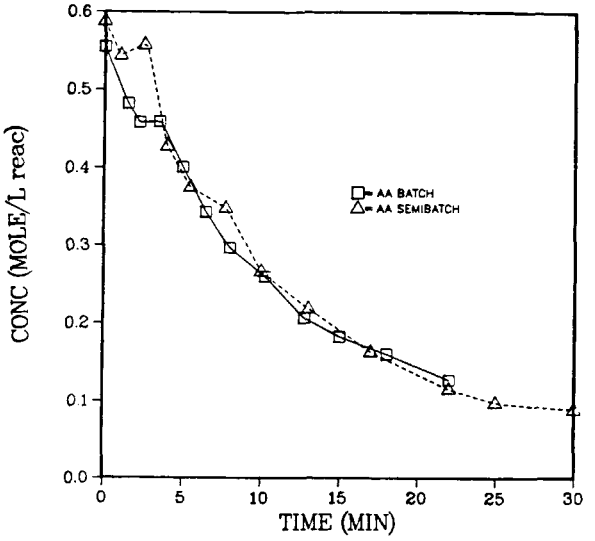

Figure 19 AA concentration for a batch and semibatch AA/styrene (40/160 g) seeded copolymerization. Thirty-five percent of the total styrene was fed continuously over a 17-min period starting at 6 min.

which accounts for the relative reactivities of the two monomers. This parameter, A, is represented by the following expression:

$$A = \frac{k_{p_{AA}}}{k_{p_{BB}}} \frac{r_B}{r_A} \frac{[M_B]}{[M_A]} \tag{71}$$

where r_1 and r_2 are the reactivity ratios of the acid and styrene, respectively, $k_{p_{ii}}$ is the propagation constant for monomer i, and $[M_i]$ is the concentration of monomer i. The rate of reaction of AA in the particles was calculated as a function of parameter A with the results given in Figure 20. Low values of A were obtained only when styrene was essentially depleted. The value of parameter A in the semibatch run corresponding to the time of continuous styrene feed was about 1000. Therefore, the styrene was probably reacting with AA in the particles, but due to the relative reactivities of the two monomers, the AA reaction rate was not noticeably increased as originally expected. The concentration of styrene in the particles must be very low in order to obtain a low value of A and a significant increase in the AA particle phase reaction rate. However, if the concentration of styrene in the system is too low, the oligomeric radicals may be so hydrophilic that they tend to remain in the aqueous phase.

Another factor that may inhibit the hydrophilic oligomers from entering the polymer particles is the presence of a hydrophilic coating of polymer that may surround the particles, especially after most of the styrene has reacted. Muroi,[2] Sakota and Okaya,[5]

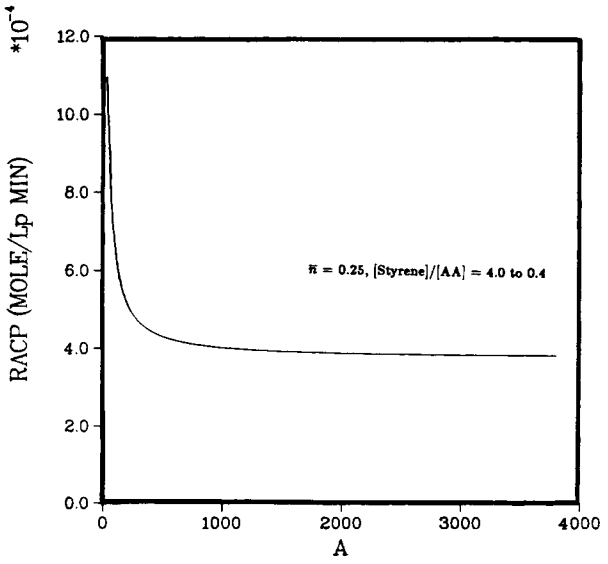

Figure 20 Dependence of AA reaction rate in the particles on the parameter A.

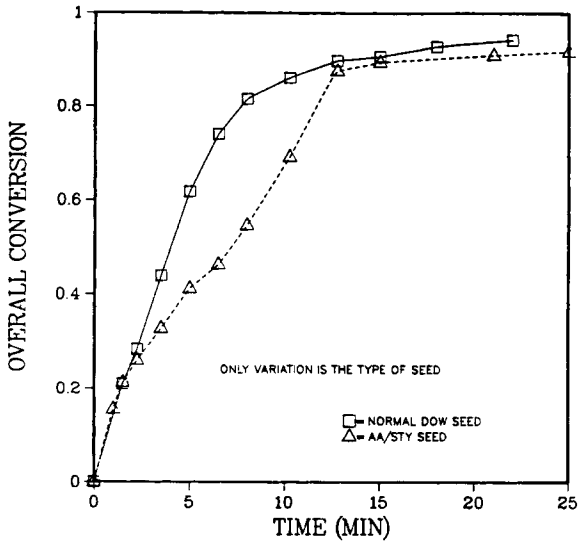

Figure 21 Effect of type of seed particles on the polymerization rate of the AA/styrene (40/160 g) system.

Egusa and Makuuchi,[7] and others have clearly shown that carboxyl groups concentrate on the particle surface in acid–styrene reactions, especially when AA is used. If this hydrophilic coating were present on the particles at the start of the reaction, it may tend to decrease the overall reaction rate even when high concentrations of styrene are present.

Two AA–styrene (40/160) copolymerizations were performed in series to test this assertion. The initial reaction was carried to essentially complete conversion over a 3-h period. The final product was then used as seed for the second AA–styrene (40/160) copolymerization. The same reaction conditions including the same number of particles were used in both reactions. The objective was to try to start the second reaction with particles that had a high degree of hydrophilic polymer already coated onto the shell of the particles and observe whether the overall reaction rate was subsequently decreased. If the coating on the particles has no effect, the second reaction should be somewhat faster due to the larger seed particle size, since a larger particle size should lead to both a larger $\bar{n}$ and a greater swelling of the particles with monomer[28] and thus a greater concentration of monomer inside the particles where the reaction is usually highest. The overall conversion data exhibited in Figure 21 for an AA–styrene run with normal seed particles is compared to overall conversion data obtained with the larger "AA–styrene" seed particles.

The reaction rate for the run with the AA–styrene seed particles is actually somewhat lower than the run with the normal seed particles suggesting that

the hydrophilic shell of polymer around the polymer particles may have inhibited the diffusion of oligomer radicals into the particles even though high concentrations of styrene were still present in the system.

The emulsion copolymerization model was modified to account for interval IV in the AA–styrene reaction. Once the conversion of styrene exceeded 0.999, all reaction in the particles was set to zero and only reaction in the aqueous phase was assumed to be significant. Partition calculations were made on the assumption that the amount of residual styrene was negligible. Therefore, only the partition of acid between the particle and aqueous phases was calculated. Results from the model, shown in Figures 22, 23, and 24 for the 20/180, 40/160, and 70/130 monomer ratios, respectively, reveal that interval IV calculations produce a much better match to the experimental data than when particle phase reaction of AA is included, as shown earlier for the 40/160 monomer ratio in Figure 9. However, the efficiency factor for radical formation had to be adjusted to 0.1 during the interval IV calculations to get the best fit of the data for all three runs.

The predicted and experimental results for both AA and styrene agree fairly well for the 20/180 and 40/160 recipes. The model predicts the styrene conversion behavior fairly well for the 70/130 recipe. However, the model underestimates the reaction rate of AA for this acid/styrene ratio. The AA monomer utilizes a more complex reaction mechanism than the MAA monomer. Since a large fraction of the total monomer in the 70/130 recipe is comprised of AA, complexities in the AA reaction mechanism, which are not included in the present model, may contribute more significantly to the large disagreement in the predicted and experimental AA conversion-time results for this recipe than for the other recipes that utilized a smaller fraction of AA.

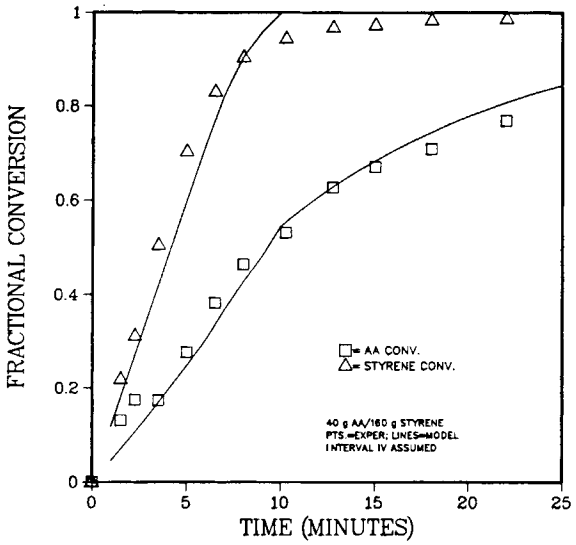

Figure 23 Model prediction of an AA/styrene (40/160 g) seeded copolymerization assuming that particle-phase reaction rates are negligible during interval IV.

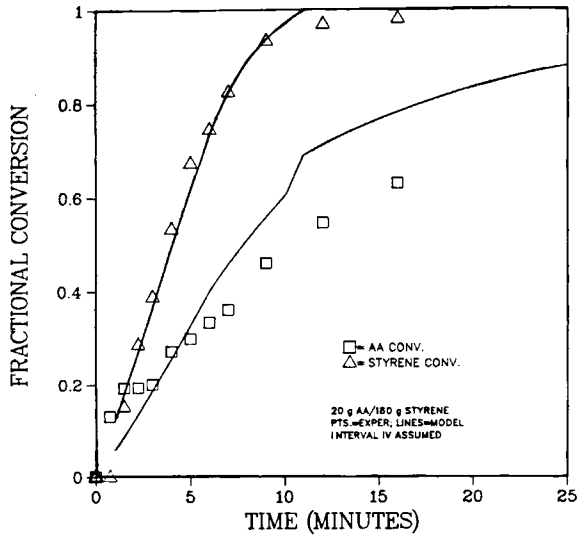

Figure 22 Comparison of predicted and experimental conversion behavior for a seeded, batch AA/styrene (20/180 g) copolymerization assuming that particle-phase reaction rates are negligible during interval IV.

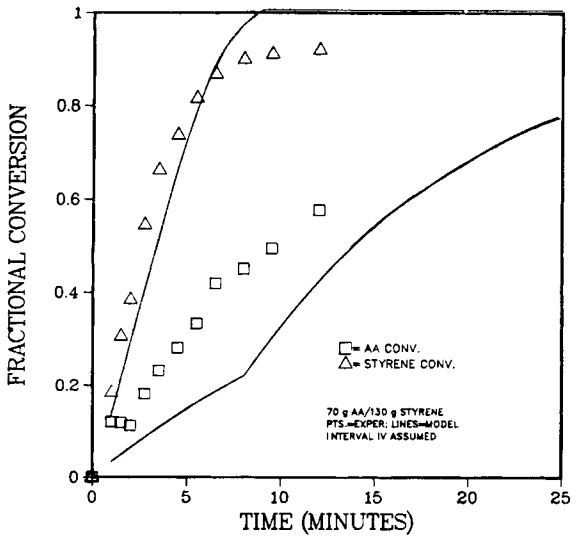

Figure 24 Comparison of predicted and experimental conversion behavior for a seeded, batch AA/styrene (70/130 g) copolymerization assuming that particle-phase reaction rates are negligible during interval IV.

Typical predicted rates of reaction of styrene in the particle phase and AA in both the particle and aqueous phases for the AA/styrene 40/160 recipe are exhibited in Figure 25. Though the values differ, the trends are the same for the other recipes examined in this work. There is a sharp increase in the predicted aqueous-phase reaction rates of AA and a sharp decrease in the predicted particle phase reaction rates at the beginning of interval IV. This sharp transition reflects the assumption that the reaction rates inside the particles become zero during interval IV (after the styrene conversion exceeds 99.9%) and that all of the reaction occurs in the aqueous phase. The actual system probably exhibits a much smoother transition of the primary reaction locus from the particle to the aqueous phase. However, since parameters such as $\bar{k}_c$, $\bar{k}_{des}$, $\bar{n}$, and the monomer partition will all be affected during this transition, the complexity of the system makes it extremely difficult to attempt to quantify all of these changes. Additionally, experimental verification of the predicted changes in each of these variables would be very onerous. Therefore, a step transition was implemented in the calculation when advancing from interval III to interval IV.

The decrease in reaction rate of AA after most of the styrene in the reactor has been depleted may be due in part to a decrease in the hydrophobicity of the oligomer radicals. It may also be due to the presence of a hydrophilic polymer coating, which surrounds the polymer particle and inhibits the penetration of hydrophilic oligomeric radicals into the particle core where additional reaction could occur.

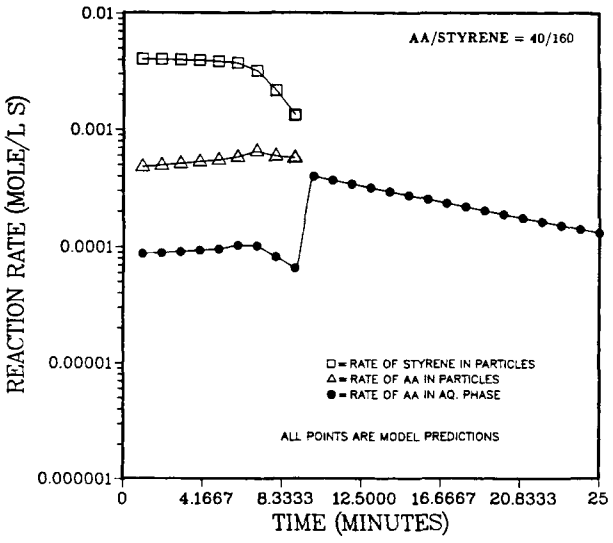

Figure 25 Predicted reaction rates of AA and styrene as a function of time for an acid/styrene ratio of 40/160.

Both explanations result in an overall decrease in the rate of diffusion of oligomer radicals and monomer into the polymer particle and a shift of the primary reaction locus into the aqueous phase. The fact that the AA reaction rate at high conversion is much slower than that expected if AA reacted significantly in both phases supports the concept of an interval IV in the AA styrene emulsion copolymerization system. Though the model presented in this work represents advances in quantitatively predicting the reaction rates of a seeded AA–styrene batch emulsion copolymerization, it is clear that this reaction system is not completely understood.

CONCLUSIONS

An overall kinetic model that includes reaction in both particle and aqueous phases has been developed for predicting batch copolymerization rates in seeded acid–styrene emulsion systems. The model utilizes thermodynamic partition equations to calculate the concentration of monomer in the aqueous, droplet, and particle phases. Radical capture coefficients are estimated from experiment, and radical desorption coefficients may be calculated using a model developed for copolymerization by Nomura et al.[10] The kinetic model predicts the MAA–styrene conversion-time behavior quite well for a range of initial monomer concentrations. The model results in good predictions of the AA–styrene conversion-time behavior until the point where the styrene is almost entirely consumed. The predicted reaction rate of AA then exceeds the experimental rate.

The primary reaction locus in the AA–styrene system may shift into the aqueous phase after the styrene has been consumed. This shift in the primary reaction locus may be attributed to two main effects: (i) the increase in hydrophilicity of the oligomeric radicals due to depletion of styrene, which decreases the driving force for the radicals to penetrate into the hydrophobic particle core, and (ii) the potential barrier for penetration of these oligomeric radicals due to a buildup of polyAA on the surface of the polymer particles. Modification of the overall kinetic model to account for interval IV behavior leads to better predictions of the conversion-time behavior for the AA–styrene system.

Funding for this work was provided by Dow Chemical, Midland, Michigan, and the National Science Foundation under Grant No. CBT-8717926.

NOMENCLATURE

A	parameter relating the relative reactivities of monomer i and monomer j
$c_{m_{ij}}$	chain transfer constant of oligomer i with monomer j
CMC	critical micelle concentration (mol/L_{aq})
d_p	particle diameter (cm)
D_w	diffusion coefficient of monomer in water (cm^2/s)
D_p	diffusion coefficient of monomer in polymer (cm^2/s)
f	initiator efficiency factor
$I_m(a)$	Bessel function
$[I]$	initiator concentration (mol/L)
j_{cr}	critical chain length for oligomers at which capture is likely to occur
$\bar{k}_a$	rate coefficient for absorption of radicals by particles (1/s)
$\bar{k}_c$	average radical capture coefficient (cm^3/s)
k_d	initiator decomposition rate coefficient (1/s)
$\bar{k}_{des}$	average radical desorption coefficient (1/s)
k'_{des}	volume-independent desorption coefficient (cm^2/s)
k_I	initiation constant of monomer from initiator radicals (L/mol s)
k_p	propagation constant (L/mol s)
$k_{p_{ij}}$	propagation constant of monomer i with monomer j (L/mol s)
k_t	termination constant (L/mol s)
$\bar{k}_{tij}$	average termination constant of radical i with radical j (L/mol s)
k_{tr}	monomer chain transfer constant (L/mol s)
k_{tw}	termination constant in the aqueous phase (L/mol s)
$[M]$	concentration of monomer (mol/L)
m	dimensionless parameter used in calculating $\bar{n}$
m_{di}	partition coefficient of monomer i between the particle and aqueous phases
$\bar{n}$	average number of free radicals per particle
N_A	Avogadro's number (6.02×10^{23}/mol)
N_n	number of particles containing n free radicals
N_p	concentration of polymer particles (no./L_{aq})
r_i	reactivity ratio = k_{pii}/k_{pij}
R_c	rate of capture of oligomer radical by particles (mol/L_{aq} s)
R_i	rate of initiation (mol/L_{aq} s)
R_p	rate of polymerization (mol/L_{aq} s)
SDS	sodium dodecyl sulfate (anionic surfactant)
T	temperature (°C)
t	time (s)
V	volume (cm^3)
Y	dimensionless parameter used in calculating $\bar{n}$

Greek Symbols

α_n	dimensionless parameter used in calculating $\bar{n}$
α'_n	dimensionless parameter used in calculating $\bar{n}$
ρ_a	rate of absorption of radicals into particles (1/s)
ρ_i	rate of generation of free radicals in the aqueous phase (mol/L_{aq} s)

Subscripts

aq	aqueous phase
A	monomer A (acid)
B	monomer B (styrene)
I	initiator
m	monomer
p	polymer or particle phase
P	polymer or copolymer
T or tot	total
w	water or aqueous phase

REFERENCES

1. R. G. Fordyce and G. E. Ham, *J. Am. Chem. Soc.*, **69,** 695 (1947).
2. S. Muroi, *J. Poly. Sci.*, **10,** 713 (1966).
3. W. Ceska, *J. Appl. Poly. Sci.*, **18,** 427 (1974a).
4. W. Ceska, *J. Appl. Poly. Sci.*, **18,** 2493 (1974b).
5. K. Sakota and T. Okaya, *J. Appl. Poly. Sci.*, **21,** 1035 (1977).
6. B. R. Vijayendran, *J. Appl. Poly. Sci.*, **23,** 893 (1979).
7. S. Egusa and K. Makuuchi, *J. Poly. Sci.*, **20,** 863 (1982).
8. S. P. Gasper and J. S. Tan, in *Water Soluble Synthetic Polymers: Properties and Behavior,* ed. P. Molyneux, Vol. I, CRC Press, Cleveland, OH, 1983.
9. F. L. Martin and A. E. Hamielec, *J. Appl. Polym. Sci.*, **27,** 489 (1982).
10. M. Nomura, K. Yamamota, I. Horie, and K. Fujita, *J. Appl. Polym. Sci.*, **27,** 2483 (1982).
11. J. Ugelstad and F. K. Hansen, *Rubber Chem. Tech.*, **49,** 536 (1976).

12. R. N. Mead, Ph.D. Thesis, School of Chemical Engineering, Georgia Institute of Technology, Atlanta, GA (1987).
13. W. V. Smith and R. H. Ewart, *J. Chem. Phys.*, **16,** 592 (1948).
14. J. Ugelstad, P. C. Mork, and J. O. Aasen, *J. Polym. Sci. A-1,* **5,** 2281 (1967).
15. J. Ugelstad and P. C. Mork, *Br. Polym. J.*, **2,** 31 (1970).
16. M. Nomura, M. Harada, K. Nakagowara, W. Eguchi, and S. Nagata, *J. Chem. Eng. Jpn.*, **4,** 160 (1970).
17. M. Nomura, M. Harada, W. Eguchi, and S. Nagata, *J. Appl. Polym. Sci.*, **15,** 675 (1971).
18. M. Nomura, H. Kojima, M. Harada, W. Eguchi, and S. Nagata, in *Emulsion Polymerization,* ed. I. Piirma and J. C. Gardon, *ACS Symposium Series,* **24,** 102 (1976).
19. H. C. Lee, Ph.D. Thesis, School of Chemical Engineering, Georgia Institute of Technology, Atlanta, GA (1985).
20. C. S. Chern, Ph.D. Thesis, School of Chemical Engineering, Georgia Institute of Technology, Atlanta, GA (1987).
21. D. C. Sundberg, J. Y. Hsieh, S. K. Soh, and R. F. Baldus, in *Emulsion Polymers and Emulsion Polymerization,* ed. D. R. Basset and A. E. Hamielec, ACS Symposium Series (1981).
22. G. L. Shoaf, Ph.D. Thesis, School of Chemical Engineering, Georgia Institute of Technology, Atlanta, GA (1989).
23. R. G. Gilbert and D. H. Napper, *JMS - Rev. Macromol. Chem. Phys.*, **c23,** 127 (1983).
24. P. J. Feeney, Ph.D. Dissertation, Department of Physical Chemistry, University of Sydney, Sydney, Australia (1986).
25. F. K. Hansen and J. Ugelstad, *J. Polym. Sci.: Poly. Chem. Ed.*, **16,** 1953 (1978).
26. B. S. Hawkett, D. H. Napper, and R. G. Gilbert, *J. Poly. Sci: Polym. Chem. Ed.*, **19,** 3173 (1981).
27. J. Brandrup and E. H. Immergut, Eds., *Polymer Handbook,* 2nd ed., Wiley, New York, 1975.
28. L. Jansson, Masters Thesis, School of Chemical Engineering, Georgia Institute of Technology, Atlanta, GA (1983).
29. G. Blauer, *J. Poly. Sci.*, **11,** 189 (1953).
30. V. F. Gromov, N. I. Galperina, T. O. Osmanov, P. M. Khomikovskii, and A. D. Abkin, *Eur. Polym. J.*, **16,** 529 (1980).
31. V. G. Popov, D. A. Topchiev, V. A. Kabanov, and V. A. Kargin, *Vysokomol. soyed.*, **A14**(1), 117 (1972).
32. R. Z. Greenley, *J. Macromol. Sci.-Chem.*, **A14**(4), 427 (1980).
33. F. V. Loncar, Ph.D. Thesis, Emulsion Poly. Inst., Lehigh University Bethlehem, PA (1985).
34. C. R. Wilke and P. Chang, *AIChE J.*, **1**(2), 264 (1955).
35. C. W. Brown and G. A. Taylor, *J. Appl. Poly. Sci.*, **13,** 629 (1969).
36. G. L. Shoaf and G. W. Poehlein, *I.E. and C. Fundamentals,* to appear.
37. M. H. Litt, R. Patsiga, and V. T. Stannett, *J. Polym. Sci., A-1,* **8,** 3607 (1970).
38. H. Kawaguchi, Y. Ohtsuka, and Y. Sugi, *J. Appl. Polym. Sci.*, **26,** 1637 (1981).

Received March 6, 1990
Accepted May 14, 1990